AMDCC Annual Report (2011)

PI: FELDMAN, EVA LUCILLE
Project Title: Mitochondrial SOD as a Target for Diabetic Neuropathy
Grant Number: U01 DK076160

Abstract: In response to the request for applications DK-05-011, entitled Animal Models of Diabetic Complications Consortium (AMDCC), the Investigators from the current AMDCC Neuropathy Phenotyping Core are proposing to develop 2 new mouse models of diabetic neuropathy (DN) targeting the biochemical pathways of oxidative stress. Our general strategic approach is to accelerate glucose-mediated oxidative injury in neurons in genetic models of type 2 diabetes. While many gene products participate in this process, we will concentrate on targeting 2 enzymes involved in superoxide detoxification: mitochondrial superoxide dismutase 2 (SOD2) and catalase. Our initial approach will concentrate on developing 2 Cre-loxP models on a susceptible genetic background. In parallel, we propose 2 hypothesis-driven specific aims for discovering the basic pathophysiologic mechanisms underlying DN. Aim 1 will test the hypothesis that decreased catalase activity in sensory neurons will make these neurons more susceptible to glucose-mediated injury. Aim 2 will test the hypothesis that animal models with DN have morphological and biochemical markers of increased oxidative stress in the peripheral nervous system. Information gained from this application will lead to new insights into the pathogenesis of DN and allow for the development of more relevant murine models of this disabling complication. Relevance to Public Health: 20 million Americans are diabetic and the incidence is increasing by 5% each year. Although DN is a common and highly morbid condition, there are no treatments for DN outside of control of the diabetic condition itself. Our studies will identify cellular targets for treatment of DN and have the potential to benefit all patients with diabetes.

Program Accomplishments:

Hypothesis

We continue to investigate the damaging effects of diabetes-induced oxidative stress on the nervous system. Our primary goal is examining the onset and progression of diabetic polyneuropathy (DPN). This Progress Report begins by describing the final phenotyping of the mice produced for us by Jackson Laboratories as part of our AMDCC proposal. We then turn to our recent new data focused on

The phenotype of the tissue specific SOD2 knockout mice on the BKS background (BKS.Cg- Lepr<db> Sod2<tm1Shs> Tg(Nes-cre)1Kln/J) .

Introduction

Oxidative stress and mitochondrial dysfunction are implicated in the pathogenesis of DPN. Even though it is unclear whether oxidative stress is a major cause or merely a consequence of cellular dysfunction associated with neurodegenerative disease [1], evidence implicates impaired mitochondrial energy production and increased mitochondrial oxidative damage in early pathological events leading to neurodegeneration [2]. Mitochondrial manganese superoxide dismutase (MnSOD or SOD2) is thought to play an important role in cellular defense against oxidative damage by reactive oxygen species (ROS) because mitochondria are a major source of ROS production and a major target of ROS induced cellular injury [3]. Complete loss of SOD2 results in embryonic or early postnatal lethality that varies

among genetic backgrounds such as CD-1[4], C57BL/6 [5], C57BL/6 and 129/Sv [6], and DBA/2J [7].

Our initial aim was to examine the effect of a targeted SOD2 deletion in the sensory nervous system on the progression of neuropathy in a type 2 model of diabetes (BKS dbdb mice). We sent B6.SOD2<loxp> mice to Jackson Labs, where they crossed the B6.SOD2<tm1Shs> to Jackson stock #000642- BKS.Cg-Dock7<m> +/+ Lepr<db>/J. Using speed congenic technology to allow for more rapid backcrossing to a different strain, this was followed by 4 additional backcrosses to stock 000642- BKS.Cg-Dock7<m> +/+ Lepr<db>/J (generation = N5), insuring that the X and Y chromosomes were of BKS origin. These mice were intercrossed to produce mice homozygous for the SOD2<tm1Shs> mutation and heterozygous for the Lepr<db> mutation. In addition, the BKS.SOD2<tm1Shs>, db mice were mated to BKS.-Lepr<db> Tg(Nes-cre)1Kln/J mice to produce breeders that were triple heterozygotes for shipment to Michigan starting 10/2009. We refer to these triple heterozygous animals as db+/SOD2 +-/nes-cre+ (Jackson stock #007220). We also received breeders homozygous for the SOD2<tm1Shs> mutation and heterozygous for the Lepr<db> mutation. We refer to these animals as db+/SOD2 - - (Jackson stock #007210).

Our mating scheme was to mate db+/SOD2 +-/nes-cre+ mice with db+/SOD2 - - mice to produce the animals of interest. We intended to study the following groups: dbdb/SOD2- -/cre+, dbdb/SOD2- -/cre-, db+/SOD2- -/cre+, db+/SOD2- -/cre-. To our surprise, after several litters were born and genotyped at weaning age, we realized there were no pups with the following genotypes: db+/SOD2--/cre+, dbdb/SOD2--/cre+, or ++/SOD2- -/cre+ mice in our weaned litters (Note: ++/SOD2- -/cre+ refers to mice wild type (++) for the Lepr <db>). These findings lead us to suspect either neonatal or postnatal lethality. As a result of this theory, we began to check all newborn litters daily. We took tissue from all pups that died between birth and weaning age, genotyped them, and found that most pups dying between birth and weaning age were SOD2 - -/cre+. We discovered that by 10 days of age some pups began to appear very small compared to their littermates, and over the next 1-2 weeks these pups developed an abnormal gait and eventually had a more difficult time righting themselves. The pups became moribund between 15-20 days age. We euthanized the moribund pups, along with healthy littermate controls, for necropsy. Initial findings showed no gross anatomical abnormalities. We began collaborating with our ULAM veterinary pathologist to determine why these mice were dying. We had only a small number of euthanized animals per genotype and we analyzed all regardless of genotype. Our initial TEM screening of brain, sciatic and sural nerves did not reveal any obvious differences between db+/SOD2--/cre+, dbdb/SOD2--/cre+, or ++/SOD2- -/cre+ mice so we focused on the ++/SOD2- -/cre+ and ++/SOD2 + - /cre+ mice, as this would allow us to see the effects caused only by targeted deletion of SOD2 alone without any contribution from the dbdb/db+ component.

Our analyses suggested that the nestin-cre promoter did not target the SOD2 deletion as precisely to the postnatal sensory nervous system as we had hoped. The Jackson website shows for the B6.Cg-Tg(Nes-cre)1Kln/J (Jackson stock #003771) mouse that, when mated to a Rosa 26 reporter mouse (Jackson stock #003474), in addition to the expected expression in neuronal and glial cell precursors that there was additional **previously unreported β-gal expression observed in several non-neuronal tissues, including P7 and Adult heart, kidney, lung, pancreas, and testes.** This was unknown to us as the time of our AMDCC application. Besides the unexpected expression of the nestin promoter in non-neural tissues we also realized that in our postnatal mice that there was not a complete knock down of SOD2 in the peripheral nervous system. We performed IHC with an antibody against SOD2 (Enzo Life Sciences) on ++/SOD2 - -/cre + and ++/SOD2 +-/cre+ mice and observed some residual

staining in the DRG, sciatic nerve and sural nerve in the ++/SOD2 - -/cre + mice, although at a lower level compared to the ++/SOD2 +-/cre+ mice, indicating that there was not a complete knock down of SOD2 in those tissues. The only tissue examined where we observed a complete knock down of SOD2 expression in the ++/SOD2 - -/cre + mice was in the superficial cortex.

Methods and Results

For clarity in all Figures in the following Results section, we refer to ++/SOD2- -/cre+ mice as SOD2 -/- and ++/SOD2 +-/cre+ mice as SOD2 +/-.

General Physical Assessment

SOD2 -/- mice show early postnatal death between 15 and 20 days old age. The body size of the SOD2 -/- mice is half that of SOD2 +/- mice (Figure 1A) and by 10 days of age, the mice display abnormal behaviors, consisting of a wide-based gait, swaying from side to side, and frequent falling. Soon thereafter, SOD2 -/- mice develop severe convulsions and all animals die by 20 days of age (Figure 1B).

Central Nervous System Analysis

SOD2 -/- mice have widespread vacuolization of the cortical neuropil, with the most severe vacuolization present in the middle and deep cortex (Figure 2B). Lesions in the cortex are present in every SOD2 -/- mouse and are bilaterally symmetrical in location but the severity and site of the lesions varied between animals (Figure 2B). Vacuoles are located in extracellular and intracellular areas (Figure 2D, Figure 5A).

Even though different nuclei are involved in different SOD2 -/- mice, spongiform encephalopathy lesions are bilaterally symmetrical within the same mouse brain stem nuclei. Lesions are most often found in the pons and medulla and are generally most severe in the nuclei near the ventral midline (Figure 3). Spongiform vacuolization is also present in the neurophil and within cells (Figure 3F).

Electron microscopy reveals both extracellular and intracellular changes in the brain of SOD2-/- mice (Figure 4). Consistent with the light microscopy and neurofilament staining (Figure 5B), rare neurons are compressed by extracellular vacuoles (Figure 4A) but no vacuoles are found in neurons (Figure 5B). Intracellular edema and mitochondrial swelling are present in occasional cells (Figure 4B). Spongiform lesions containing cellular organelles and swollen mitochondria from ruptured astrocytes are common (Figure 4C). Vacuoles containing membranous profiles are also present in the extracellular neurophil (Figure 4D) and some of the vacuoles are surrounded by small myelinated fibers (Figure 5E). Occasional dying cells have hyperchromatic nuclei and dark cytoplasm adjacent to vacuoles (Figure 5F).

Immunohistochemistry of neurofilaments show vacuoles in neurophil but not within neurons (Figure 5B). However, in one animal, degenerative changes typical of hypoxic damage are present in the reticulotegmental nucleus of the pons (data not shown). While little or no astrocytosis accompanied the cortical spongiform lesions, a significant reactive astrocytosis in lesions of brainstem is noted by staining for glial fibrillary acidic protein (GFAP; Figure 5C-E). The microglia are unremarkable in the areas of spongiform change (Figure 5F).

Neither motor neuron loss nor vacuolar changes in the ventral horn of cervical and lumbar spinal cord are observed in SOD2 -/- mice (Figure 8) compared to ++/SOD2 +/- cre+ mice. Despite the targeted deletion of SOD2, motor neurons in the ventral horn region still show SOD2 immunoreactivity. Cervical spinal cord has more SOD2 immunopositive neurons (Figure 8A, 8C). Double-staining with SOD2 and Choline acetyltransferase (ChaT; motor neuron specific antibody) show SOD2 positive motor neurons (Figure 8B, 8D). The number of SOD2 positive motor neurons is 33.7% out of the total motor neurons in cervical spinal cord and 11.2% out of the total motor neurons in lumbar spinal cord (data not shown). Numbers are determined from every 4th section for a total 10 sections that are serial 16 um sections of cervical and lumbar spinal cord.

Peripheral Nervous System Analysis

No lesions are noted in peripheral nerves by light microscopy and despite targeted SOD2 deletion, nerve fibers in the dorsal root ganglion, sciatic nerve, and sural nerve region had sparse but present SOD2 immunoreactivity (data not shown). However, electron microscopy reveals prominent changes in the distal nerves. In SOD2 -/- mice, myelin and Schwann cell degeneration is present in both sciatic and sural nerves (Figure 6B, 6D).

General tissue analysis

As expected (due to the targeted nature of the SOD2 deletion), light microscopic analyses of serial sections of the heart, liver, and skeletal muscle from both SOD2 -/- and SOD2+/- mice reveal no abnormality. Liver from both groups is normal with no evidence of steatosis (Figure 7A, 7B). The hearts from SOD2 -/- mice have a normal ventricular size and a normal thickness of the interventricular wall (Figure 7C). Histology of cardiac muscle is normal with no evidence of degeneration, atrophy, or hypertrophy (Figure 7D). Both SOD2+/- and SOD2 -/- skeletal muscles also have a normal structure.

Summary

The present study shows that spongiform vacuolization and mitochondrial damage in the central nervous system of SOD2 - - /cre+ mice results in early death. The likely cause of death is cardiac arrest and/or arrhythmias secondary to continuous convulsions. Because all homozygous SOD2 - - /cre+ mice die by approx 20 days age, and **our initial intent** was to examine the effect of a targeted SOD2 deletion on DPN, we reasoned that if the full SOD2 knockout in targeted tissues produced such a strong deleterious effect that studying mice having only half of the amount of SOD2 in targeted tissues could be relevant to the development or progression of DPN. We are currently examining the effects of SOD + - /cre+ on the progression of DPN in BKSdbdb vs BKS db+ mice. We have only small numbers of these older mice, but we hope that by increasing our animal numbers that we may yet elucidate a role for SOD2 in the pathogenesis of neuropathy in a type 2 murine model

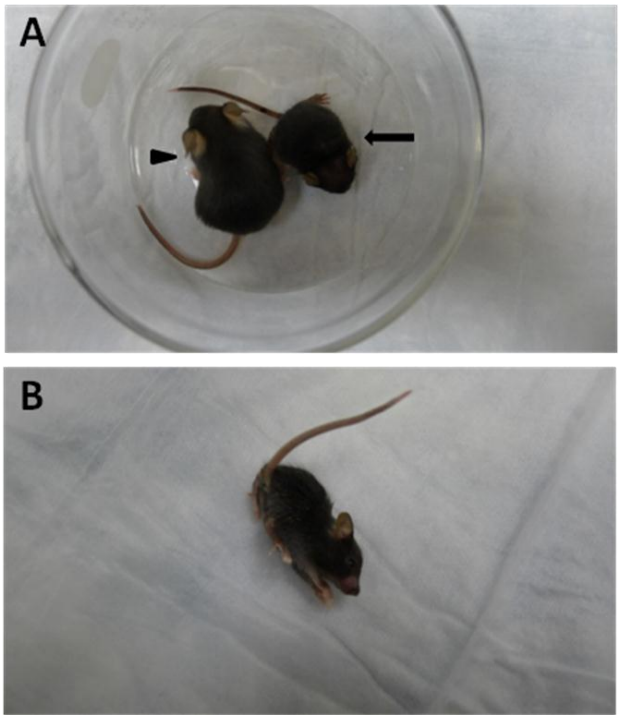

Figure 1. Physical appearance. (A) The size of the SOD2 -/- mouse (arrow) is half that of the SOD2 +/- mouse (arrow head) between 15-20 days of age. After 10 days of age, SOD2-/- mice lose body control and have difficulty righting themselves. (B) At the terminal stage mice have severe convulsions, resulting in death.

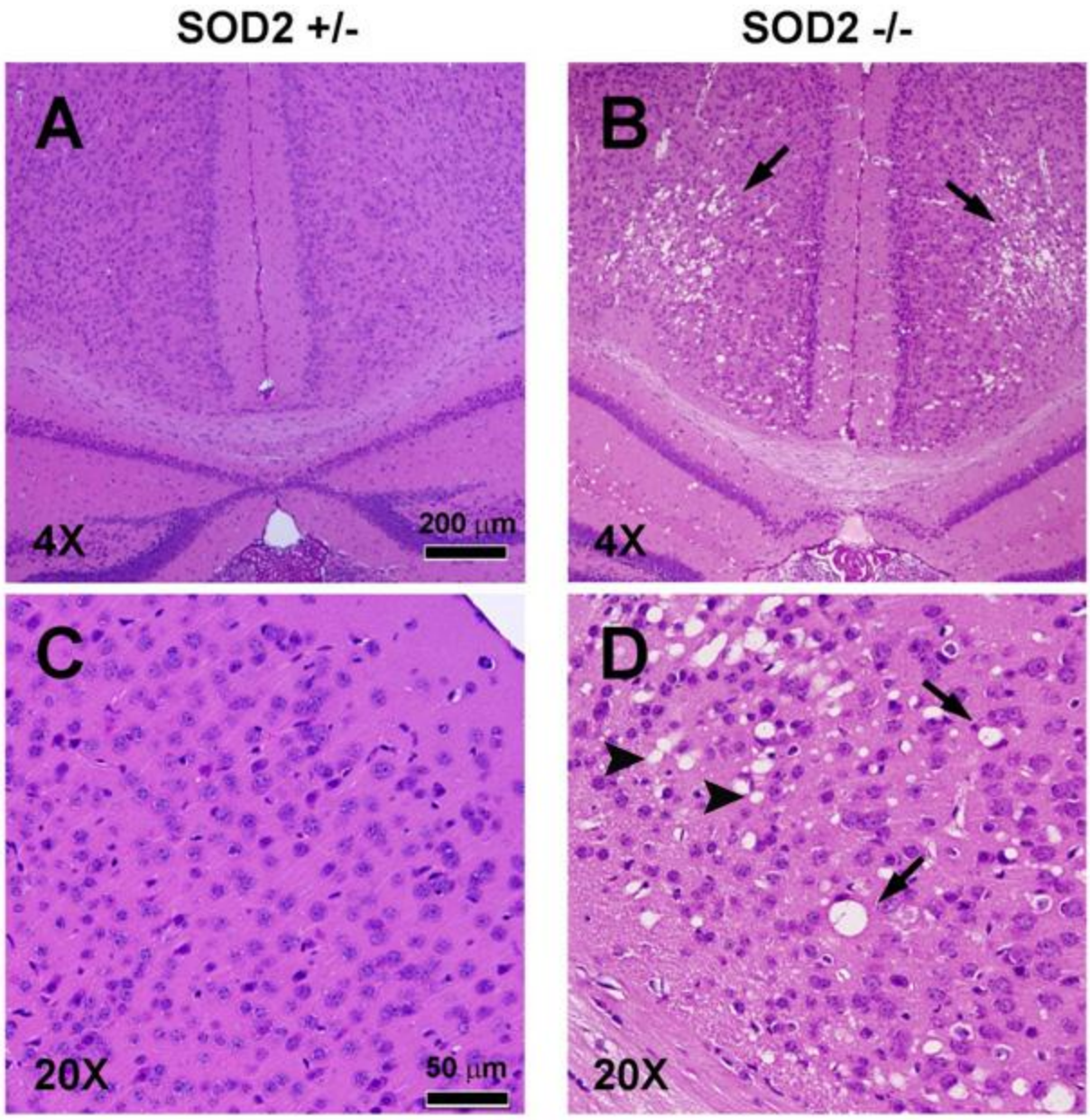

Figure 2. Spongiform degeneration in the deep cerebral cortex, H&E stain.
(A, C) SOD2 +/- mice have no specific lesions. (B) Severe spongiform degeneration of the deep cerebral cortex and mild changes in hippocampus are shown in SOD2-/- mice (arrows). The lesions are bilaterally symmetrical in location. (D) Both intracellular (arrows) and extracellular vacuoles (arrow heads) are present in SOD2-/- mice.

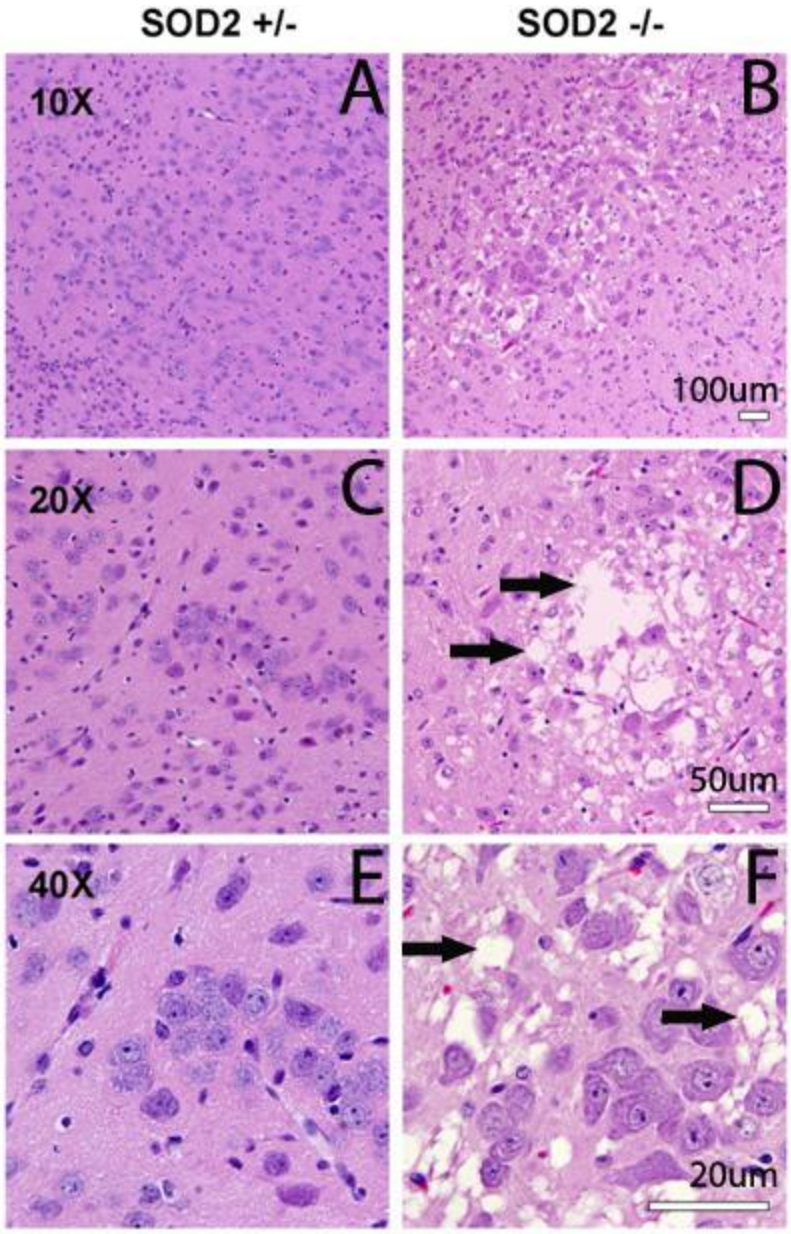

Figure 3. Spongiform degeneration in the medullary nuclei, H&E stain. (A, C, E) SOD2 +/- mice have no specific lesions. (B, D, F) Severe spongiform degeneration in the medullary nuclei is shown in SOD2 -/- mice. Arrows indicate extracellular vacuolization in nuclei with sparing of the neurons (D, F).

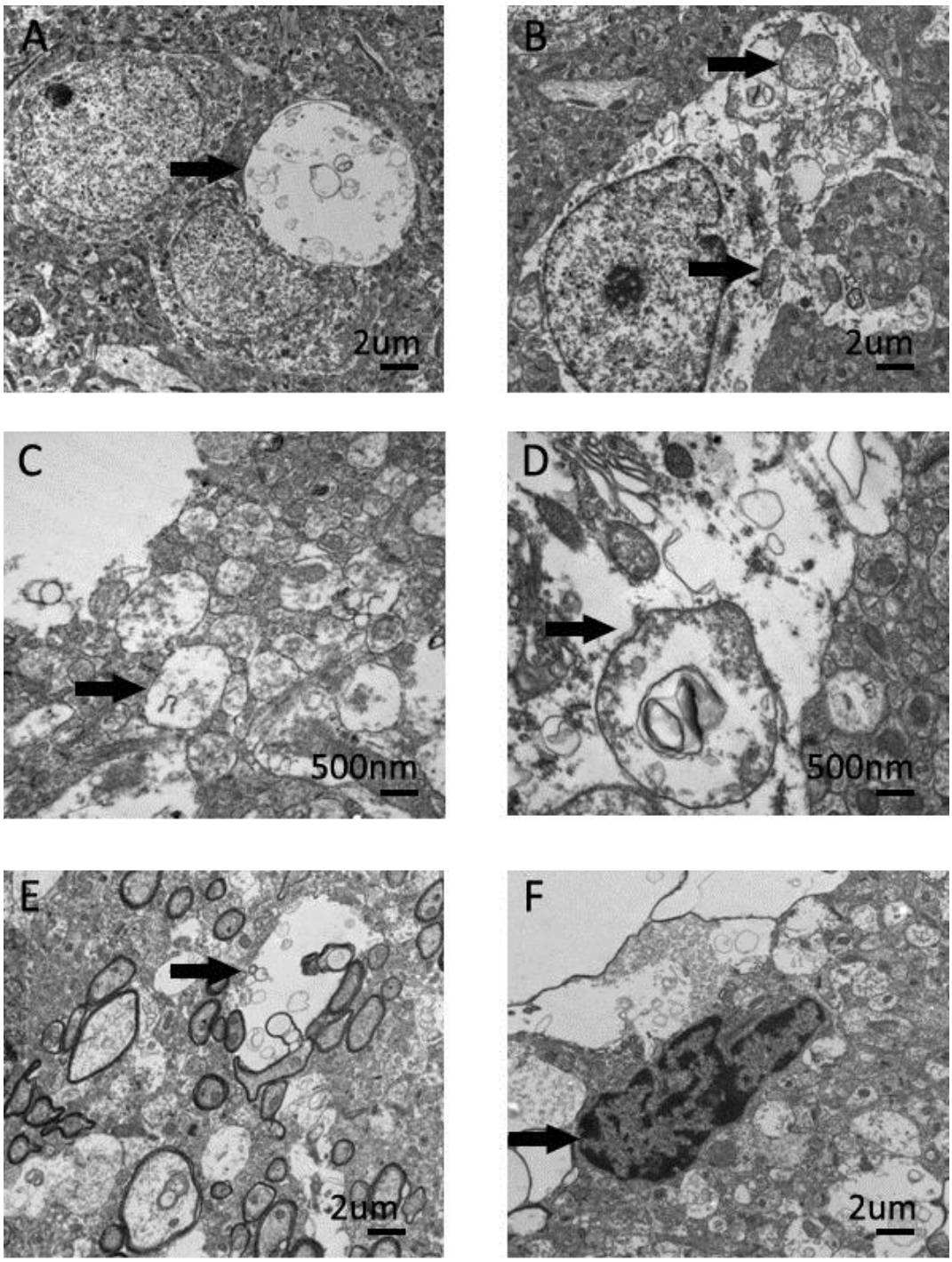

Figure 4. Ultrastructure analysis of brains from SOD2 -/- mice. (A) An extracelluar vacuole containing membranous debris (arrow) compresses a neuron. Neurons generally show no spongiform change. (B) Swollen astrocyte includes dilated and disrupted mitochondria (arrows). (C) Ruptured astrocyte has swollen mitochondria (arrow). (D) Vacuolated neurophil has cellular and membranous debris (arrow). (E) A vacuole contains membranous debris adjacent to small myelinated fibers (arrow). (F) A condensed hyperchromatic nucleus is shown in a dying cell (arrow).

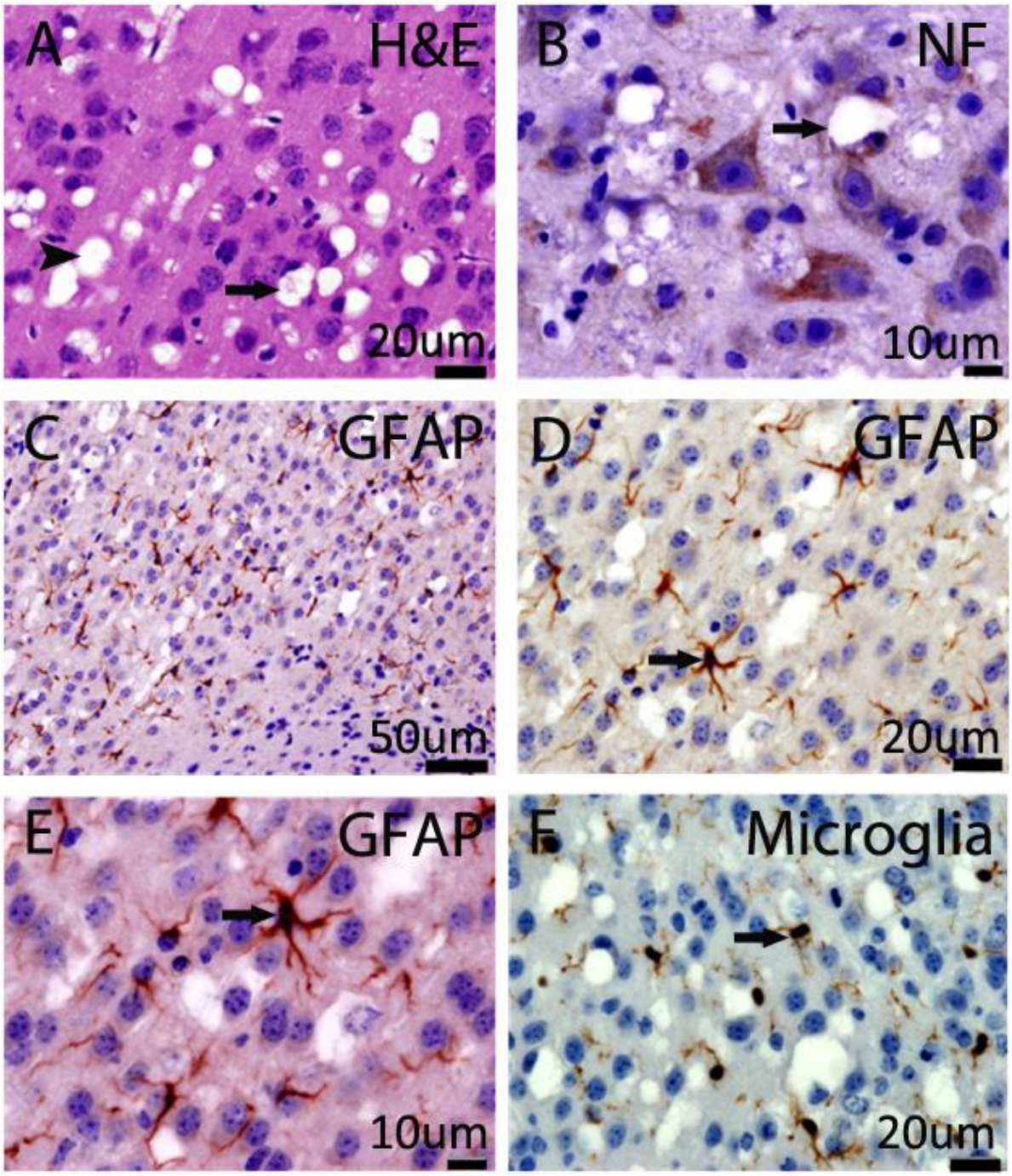

Figure 5. Immunohistochemistry of the brain and brain stem from SOD2 -/- mice.
(A) Vacuoles are present in the neurophil (arrow head) and within glial cells (arrow), H&E stain. (B) Neurofilament staining shows neurons compressed by vacuoles (arrow) in the neurophil but no vacuoles within the neurons. (C-E) Activated astrocytes stained with GFAP (arrows) are present in brain stem lesions. (F) Microglia immunoactivity is unremarkable in the lesion (arrow).

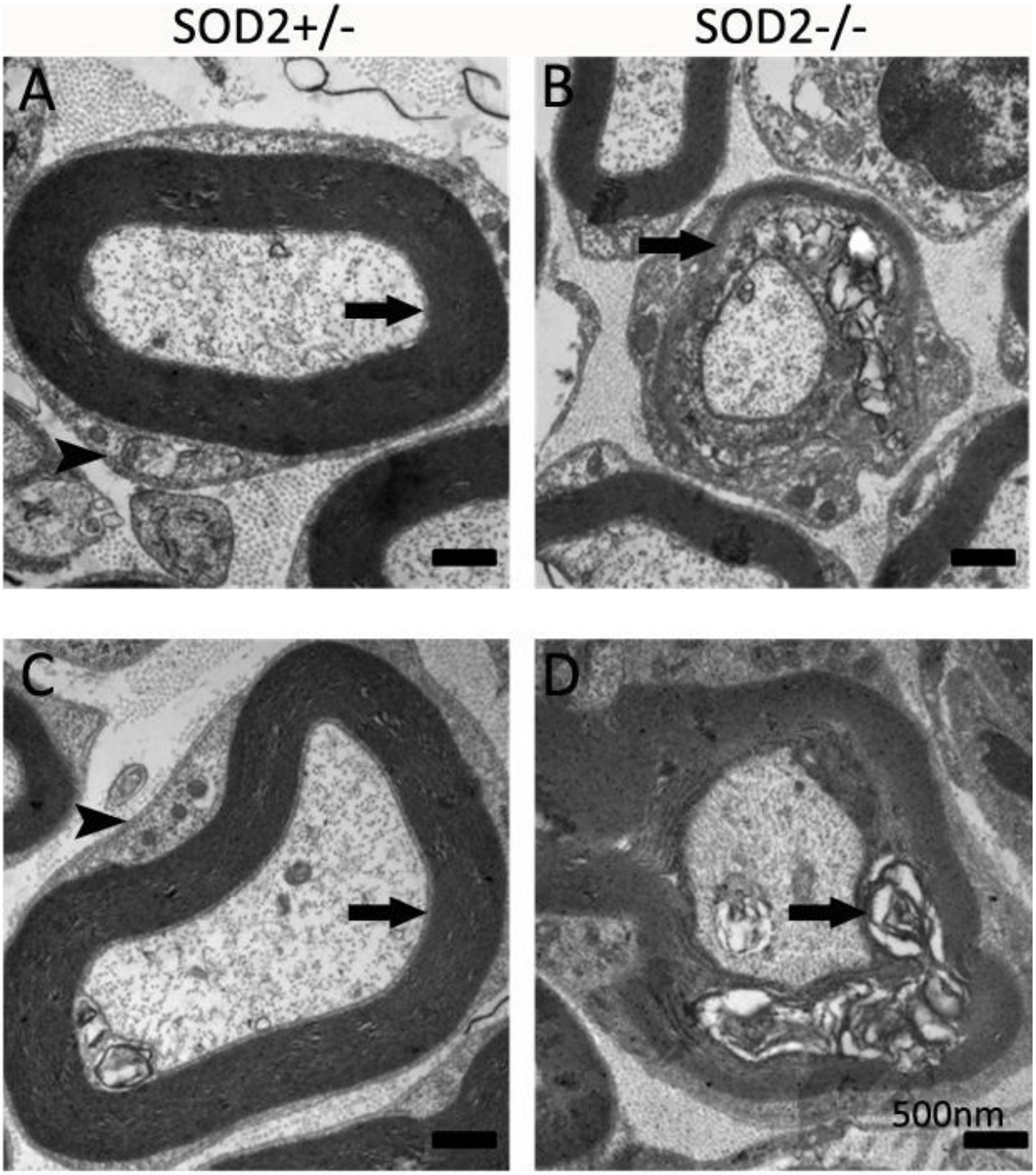

Figure 6. Ultrastructure analysis of sciatic nerve and sural nerve. (A, C) SOD2 +/- mice show normal myelin (arrows) and Schwann cell morphology (arrow heads) in sciatic nerve (A) and sural nerve (C). (B, D) SOD2 -/- mice show sciatic (B) and sural nerve (D) myelin degeneration (arrows).

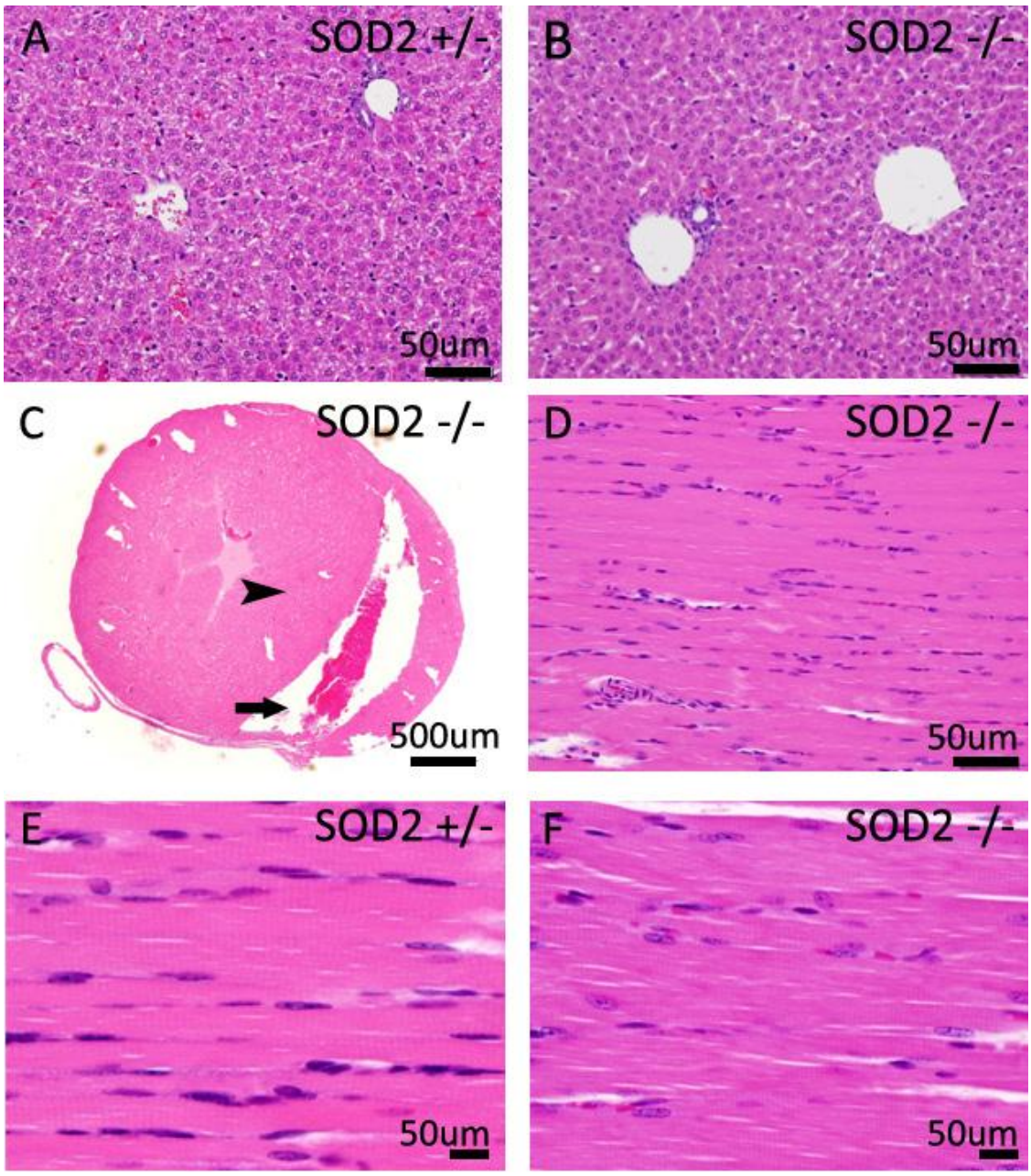

Figure 7. Morphology of liver, heart, and muscle, H&E stain. (A, B) Liver from SOD2 +/- and SOD2 -/- mice is normal with no evidence of steatosis. (C) Heart of SOD2 -/- mice shows normal size ventricles (arrow) and normal thickness (arrow head) of the walls. (D) Cardiac muscle from a SOD2 -/- mouse is normal with no evidence of degeneration, atrophy, or hypertrophy. (E, F) Skeletal muscle from SOD2 +/- (E) and SOD2 -/- (F) mice has normal structure.

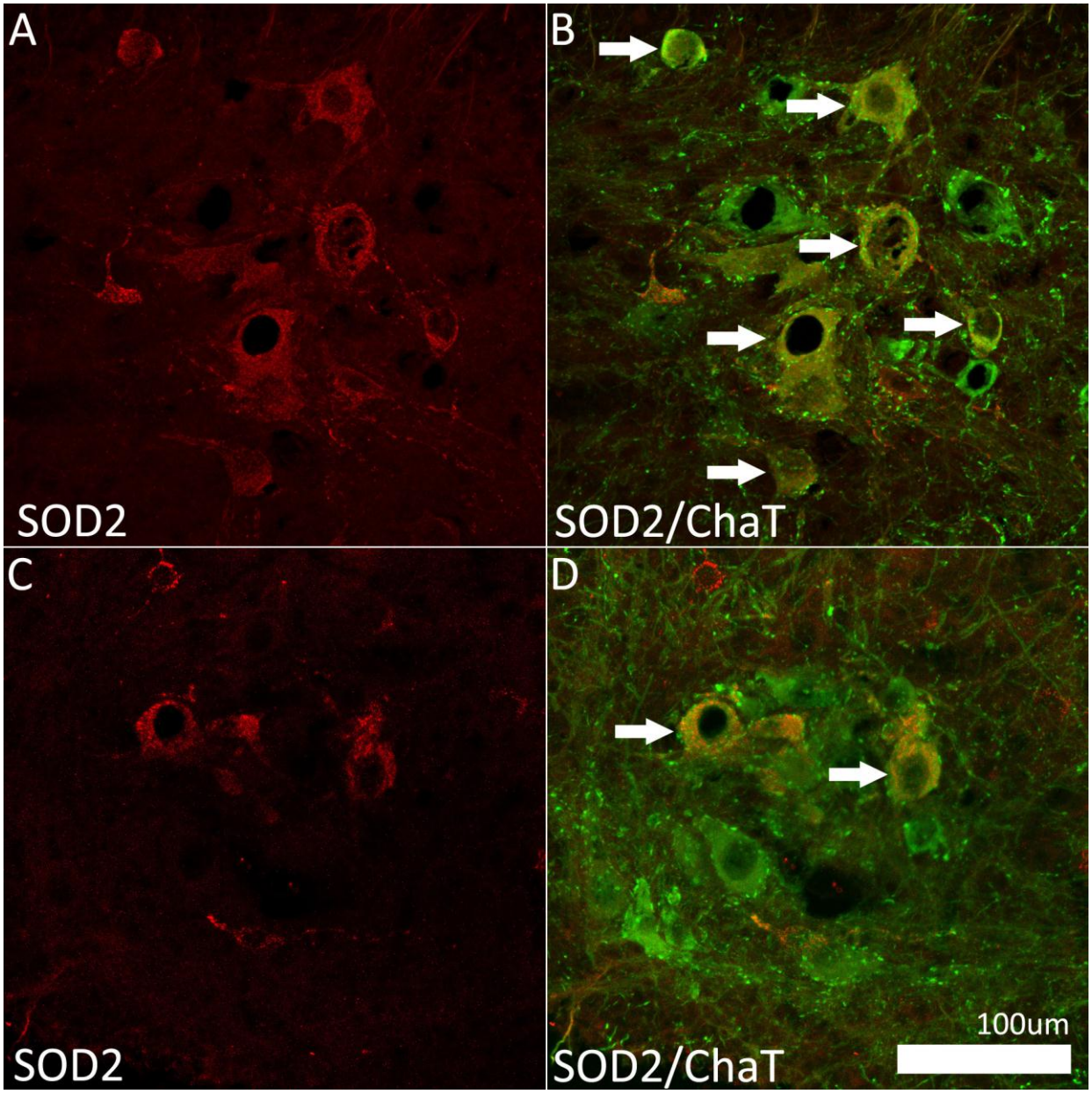

Figure 8. Differential loss of SOD2 immunoreactivity in motor neurons from SOD2 -/- mouse spinal cord. Sections from the ventral horn of the cervical cord (A, B) and lumbar cord (C, D) were double-stained with anti-SOD2 and anti-ChaT. Co-localized motor neurons from merged images are shown in B and D (arrows). (B) The cervical cord appears to have more SOD2 positive motor neurons (arrows).

Age	2month db+ (n=1)	2month dbdb (n=1)	4month db+ (n=2)	4month dbdb (n=1)	6month db+(n=1)	6month dbdb (n=1)	8month db+ (n=1)	8month dbdb(n=1)
SNCV	20	15	20/20	17	22		20	16

(m/sec)						17		
SMNCV (m/sec)	54	37	50/56	39	65	41	52	0
TSNCV (m/sec)	33	15	30/33	21	25	19	34	8
TDML sec	2	4.2	2.3/2.0	4	2.4	5.3	2.1	0
BW(g)	28.2	25.6	20.3/21.2	37.8	29.3	52	21.7	37.4
Glucose (mg/dL)	174	102	317/212	565	216	Hi	288	362

Figure 9. Nerve conduction velocity (NCV) studies from db+ SOD2+/- cre+ and dbdb SOD2 +/- cre+ over time.

References

1. Andersen JK. 2004. Oxidative stress in neurodegeneration: cause or consequence? Nat Med. Jul;10 Suppl:S18-25.
2. Beal MF. 1996. Mitochondria, free radicals, and neurodegeneration. Curr Opin Neurobiol. Oct;6(5):661-6.
3. Misawa H, Nakata K, Matsuura J, Moriwaki Y, Kawashima K, Shimizu T, Shirasawa T, Takahashi R.2006. Conditional knockout of Mn superoxide dismutase in postnatal motor neurons reveals resistance to mitochondrial generated superoxide radicals. Neurobiol Dis. Jul;23(1):169-77.
4. Li Y, Huang TT, Carlson EJ, Melov S, Ursell PC, Olson JL, Noble LJ, Yoshimura MP, Berger C, Chan PH, Wallace DC, Epstein CJ. 1995. Dilated cardiomyopathy and neonatal lethality in mutant mice lacking manganese superoxide dismutase. Nat Genet. Dec;11(4):376-81.
5. Ikegami T, Suzuki Y, Shimizu T, Isono K, Koseki H, Shirasawa T. 2002. Model mice for tissue-specific deletion of the manganese superoxide dismutase (MnSOD) gene. Biochem Biophys Res Commun. Aug 23;296(3):729-36.
6. Lebovitz RM, Zhang H, Vogel H, Cartwright J Jr, Dionne L, Lu N, Huang S, Matzuk MM. 1996. Neurodegeneration, myocardial injury, and perinatal death in mitochondrial superoxide dismutase-deficient mice. Proc Natl Acad Sci U S A. Sep 3;93(18):9782-7.
7. Huang TT, Carlson EJ, Kozy HM, Mantha S, Goodman SI, Ursell PC, Epstein CJ. 2001. Genetic modification of prenatal lethality and dilated cardiomyopathy in Mn superoxide dismutase mutant mice. Free Radic Biol Med. Nov 1;31(9):1101-10.

2. C57BL/6 mice Fed a High Fat Diet Develop Neuropathy

Introduction

Data from our patients with DPN and type 2 diabetes strongly suggest that dyslipidemia plays a role in the pathogenesis of DPN. We hypothesize that dyslipidemia augments hyperglycemic-mediated oxidative damage in the peripheral nervous system, leading to the onset and progression of DPN.

Methods and Results

We completed a study that examined the effects a high fat diet (45% kcal% fat) on peripheral nerve function in C57BL/6 mice. Our goal was to phenotype the effects of a high fat diet alone. At 36 wk age, we performed complete terminal neuropathy phenotyping, and collected tissues to explore biochemical alterations in DRG, sciatic nerve, and brain. We also collected DRG and sciatic nerve for gene expression studies. We explored aspects of diabetic nephropathy with our collaborators, Dr. Brosius and Dr. Kretzler.

Male C57BL/6 mice (Jackson Lab #000664) were purchased from Jackson Labs (Bar Harbor, ME) and started on control (LabDiet 5053) or high fat chow (Research Diets D12451) at 3 weeks of age. Mice were maintained on chow until 36 wks age. Weights and fasting glucoses were tested weekly. Terminal phenotyping was performed at 36 wks age, including impaired glucose tolerance testing, thermal tail flick response (TF), hind paw withdrawal (HP), sural sensory conduction velocity (Sural NCV) and sciatic motor conduction velocity (SMNCV).

We observed a significant increase in weight and an abnormal one hour glucose value with glucose load (glucose tolerance test) with no differences in fasting glucose or glycated hemoglobin (Figure 10). Despite the normal glycated hemoglobin, there were significant differences in both behavioral and electrophysiological measures of DPN. Thermal sensation was clearly impaired in the high fat fed mice (tail flick and hind paw withdrawal) with a corresponding pronounced reduction in the Sural NCV and SMNCV at 36 weeks of age (Figure 11). Serum samples for lipid analyses were sent to the MMPC at University of Washington and for measures of oxidative stress to our collaborator, Dr. Subramanian Pennathur. We discovered that mice fed a high fat diet for 33 weeks had significantly elevated cholesterol and, as biomarkers of oxidative stress: plasma nitrotyrosine and plasma HODE. We then examined these same markers of oxidative stress in the sciatic nerve and discovered that nerves from high fat fed animals (with normal glycated hemoglobin) have significantly higher levels of both nitrotyrosine and HODE, respective markers of protein nitration and lipid oxidation.

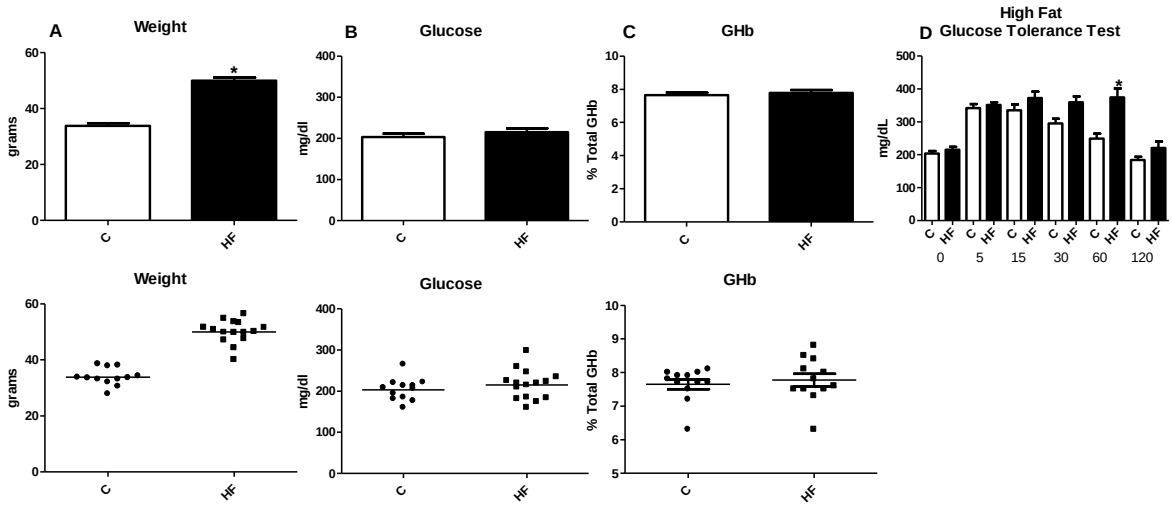

Figure 10. Metabolic data from 36 week old mice. Body weight (A) and 1 hour glucose tolerance test (D) were significantly altered in 36 week old C57BL/6 mice fed a high fat (HF) diet for 33 weeks compared to mice fed a control (C) diet, *P<.0001. A two tail t-test was used with a 95% confidence interval. Data are expressed as means±SEM.

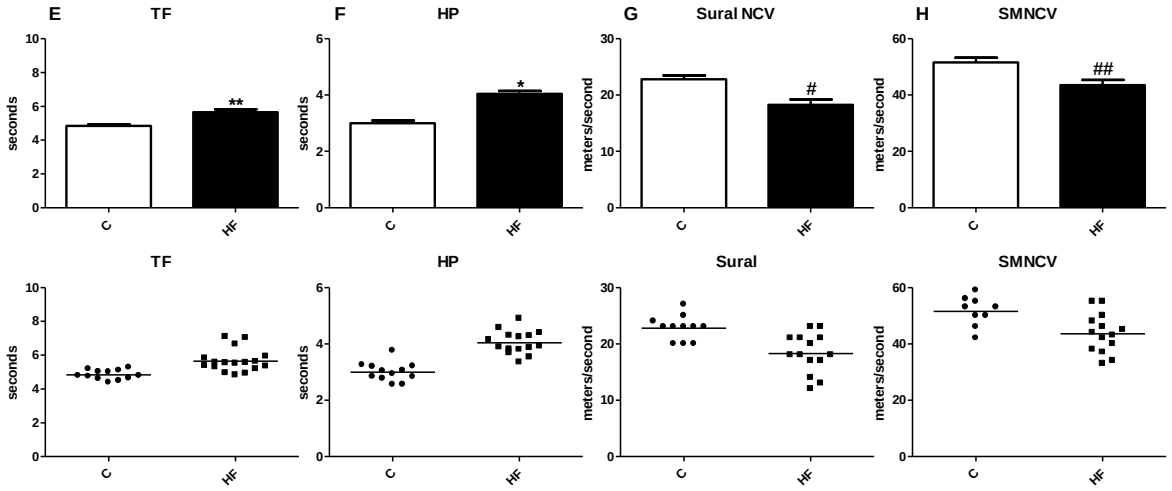

Figure 11. Neuropathy phenotyping of 36 week old mice. TF (E) and HP (F) latencies significantly increased in 36 week old C57BL/6 mice fed a high fat diet compared to mice fed a control diet, *P<.0001, **P=.0005. Additionally, there was a pronounced reduction in the Sural NCV (G) and SMNCV (H) at 36 weeks of age, #P<.001, ##P=.0076. A two tail t-test was used with a 95% confidence interval. Data are expressed as means±SEM.

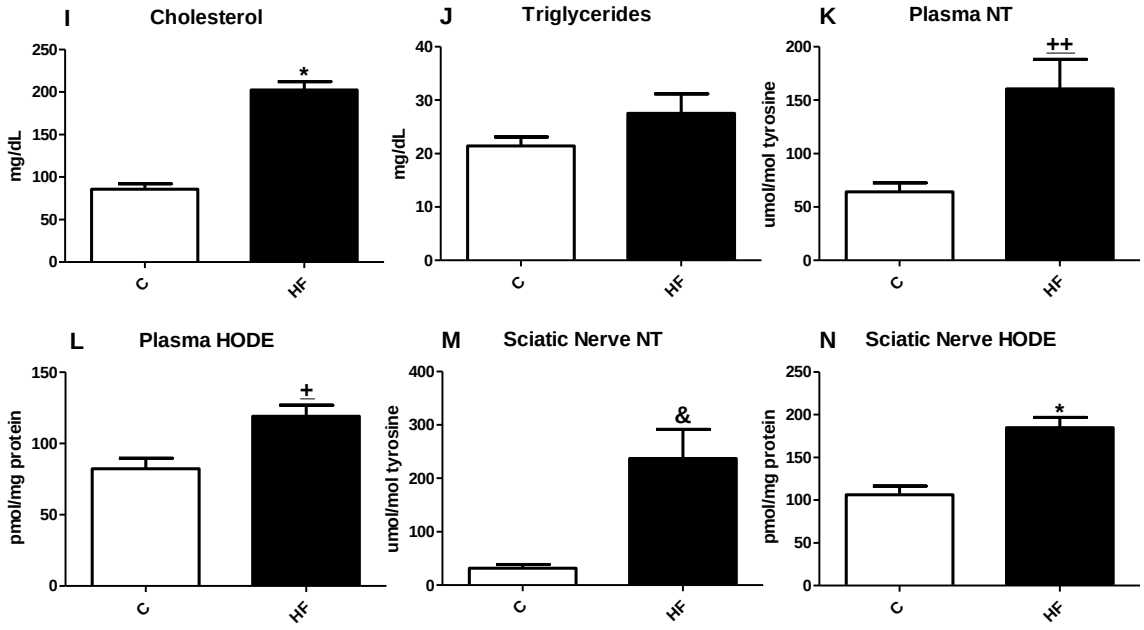

Figure 12. Plasma lipid analysis and plasma and sciatic nerve oxidative stress measures from 36 week old mice. Mice fed a high fat diet for 33 weeks had significantly elevated cholesterol (I), plasma nitrotyrosine (K), plasma HODE (L), sciatic nerve nitrotyrosine (M), and sciatic nerve HODE (N). *P<.0001, $^{\pm\pm}$P=.0029, $^{\pm}$P=.0023, $^{\&}$P=.0011. A two tail t-test was used with a 95% confidence interval. Data are expressed as means$\pm$ SEM.

Summary

Our data strongly suggest that dyslipidemia contributes to nerve damage in murine models of type 2 diabetes, confirming our clinical observations from our patient clinics. This confirmation will allow us to explore therapeutic interventions in this murine model with the goal of not only better understanding the mechanism(s) underlying nerve damage but also with the hope of fast tracking new therapies into the clinic.

Pioglitazone Study

Introduction

We completed a study on the effects of pioglitazone treatment on DPN in mice with type 1 and type 2 diabetes. Our goal was to phenotype the effects of pioglitazone on the progression of neuropathy at 20 weeks of age by performing terminal neuropathy phenotyping, including TF, HP, VF, Sural NCV and SMNCV testing, and to explore biochemical alterations in DRG, sciatic nerve, sural nerve, spinal cord, footpad and brain. We collected DRG and sciatic nerve for gene expression studies. We also explored aspects of diabetic nephropathy with our collaborators, Dr. Brosius and Dr. Kretzler, and diabetic retinopathy with our collaborators, Dr. Gardner, Dr. Antonetti and Dr. Abcouwer.

By activating the nuclear receptor, peroxisome proliferator-activated receptor gamma, pioglitazone regulates the transcription of certain genes that are insulin sensitive.

Consequently, studies have shown that pioglitazone lowers triglyceride, insulin, HbA1c and glucose levels in mice with type 2 diabetes.

Methods and Results

BKS-dbdb and db+ mice (BKS.Cg-m +/+ Leprdb/J, JAX Mice stock # 000642) were purchased from Jackson Laboratory (Bar Harbor, ME) and used as a model of type 2 diabetes. Type 1 diabetes was induced by streptozotocin (STZ) injection (150 mg/kg) to db+ mice at 5 wks. Mice were switched to a control chow (AIN76A , Research Diets D10001) or a pioglitazone chow (AIN76 chow + pioglitazone 112.5 mg pio/kg chow, Research Diets D10050301). Mice on pioglitazone chow received a final dose of 15 mg pio/kg mouse/day. Chow treatment started on all mice at 6 wks age. Weights and fasting glucoses were tested weekly. The mice were harvested at 16 wks age, earlier than the 20 wks age originally planned due to health concerns for both db+ STZ mice and dbdb pio mice. Some of the db+STZ mice became moribund at 13 wks age and the rest by 16 wks age. By 16 wks age the dbdb pio mice had become so obese that they suffered loss of skin integrity (Figure 14).

Sural NCV and SMNCV improved with pio treatment in the type 1 murine model (db+stz pio mice) compared to the mice fed control chow, however there was no effect in the type 2 model. Of interest, and as yet unexplained, SMNCV significantly decreased in nondiabetic mice fed pio chow compared to control chow (Figure 15). There was no statistical difference with treatment of a measurement of small fiber dysfunction, intraepidermal nerve fiber (IENF) density (Figure 15). Serum analyses revealed a significant decrease in triglycerides with pio treatment in both the types 1 and 2 murine models, but the remainder of measures, including assessment of oxidative stress biomarkers, did not reach statistical significance, in part because of small numbers and higher than anticipated animal to animal variability (Figures 16 and 17).

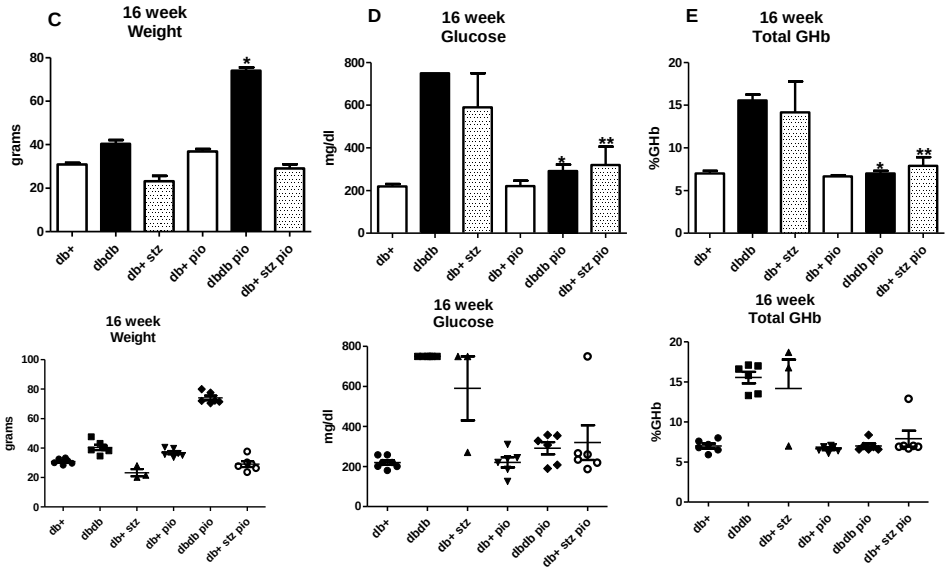

Figure 14. Metabolic data from 16 week old mice. Data represent 16 week old mice on pio chow treatment for 10 weeks. Weight was significantly increased in dbdb mice fed pio chow compared to dbdb mice fed control chow, *P<.001. Glucose and GHb levels significantly dropped in dbdb, *P<.001, and db+stz, **P<.01, mice fed pio chow when compared to the same

mice fed control chow. Statistics were analyzed using a one-way ANOVA test and a Tukey post-hoc test with a 95% confidence interval.

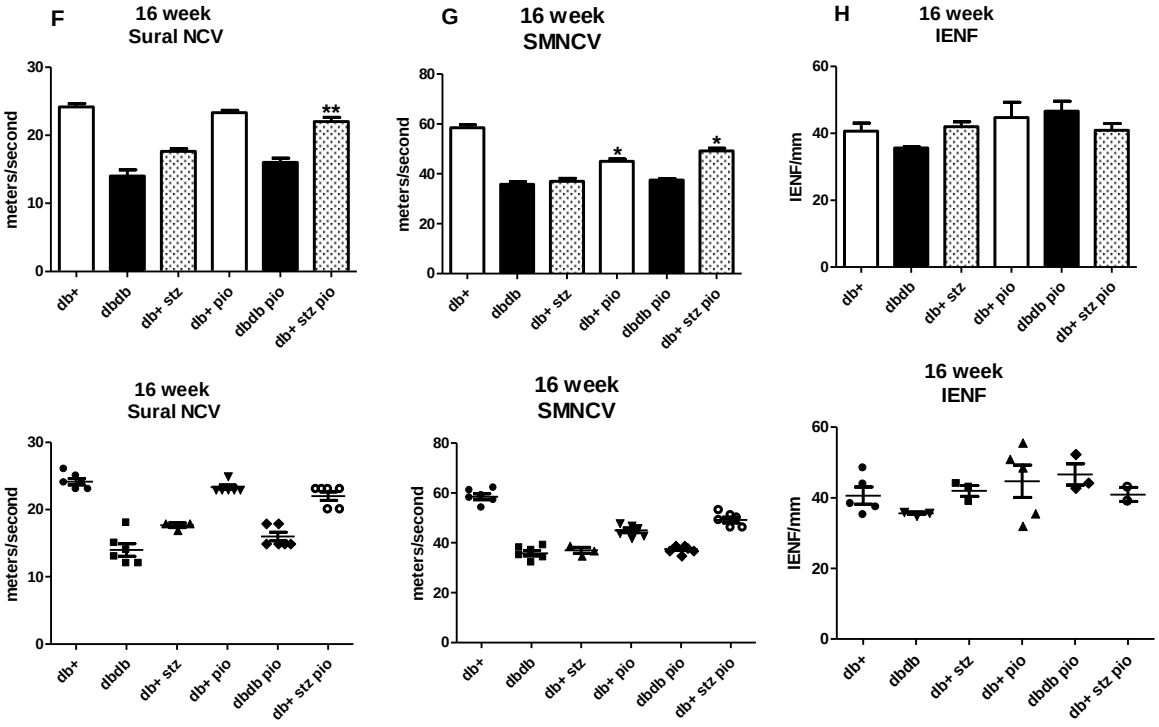

Figure 15. Neuropathy phenotyping of 16 week old mice. Data represent 16 week old mice on pio chow treatment for 10 weeks. Sural NCV was significantly faster in db+stz pio mice compared to db+stz mice fed control chow, $^{**}P<.01$. SMNCV significantly decreased in db+ pio mice, $^{*}P<.001$, when compared to the same mice fed control chow, whereas SMNCV significantly increased in db+stz pio mice, $^{*}P<.001$, when compared to the same mice fed control chow. Statistical analysis was determined using a one-way ANOVA test and a Tukey post-hoc test with a 95% confidence interval.

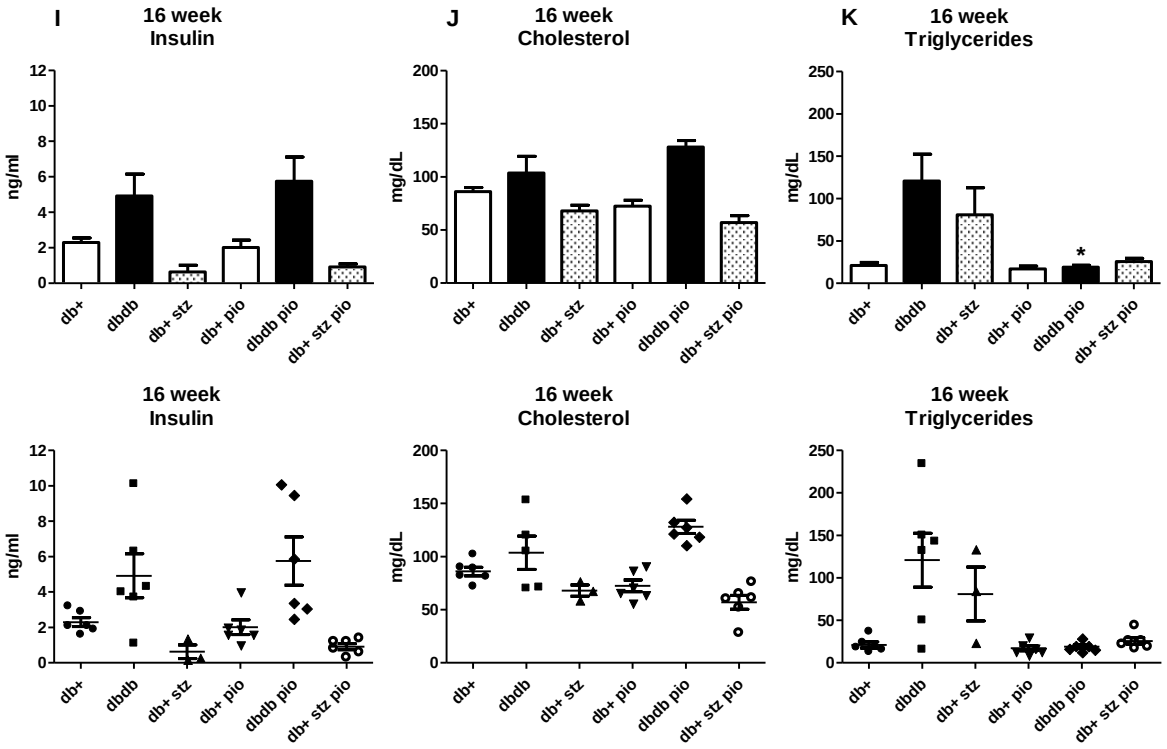

Figure 16. Plasma data from 16 week old mice. Data represent 16 week old mice on pio chow treatment for 10 weeks. Triglycerides were significantly lowered in dbdb pio mice compared to dbdb mice fed control chow, $^{*}P<.001$. Statistical analysis was determined using a one-way ANOVA test and a Tukey post-hoc test with a 95% confidence interval.

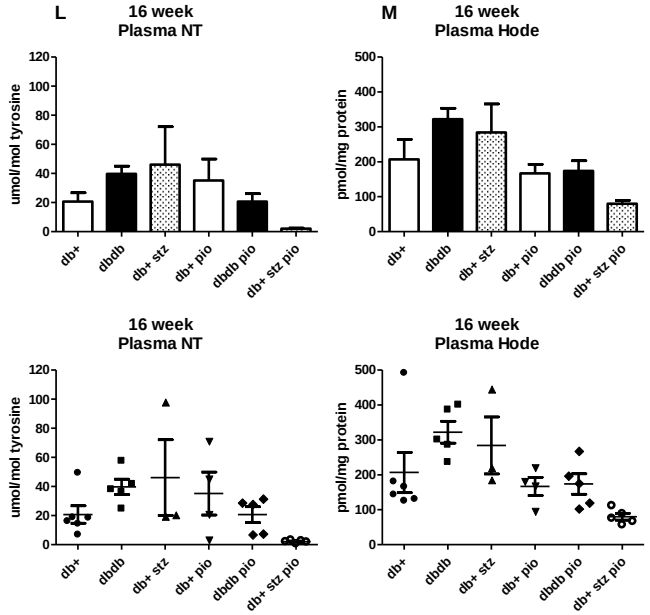

Figure 17. Plasma data from 16 week old mice. Data represent 16 week old mice on pio chow for 10 weeks.

Summary

Our data suggest that normalization of glucose and triglycerides alone are insufficient to ameliorate DPN in a murine model of type 2 diabetes. Of interest, our high fat murine model studies (discussed in the previous section) suggested that cholesterol was a primary driver of DPN, and in the type 2 murine model used in the current study, pio treatment did not normalize cholesterol. We are currently repeating this study, comparing pio treatment with a cholesterol lowering treatment, simvastatin.

We are also concerned that the early pioglitazone treatment (pio treatment began at 6 wks age, 1 wk post STZ injection) could have prevented STZ toxicity to the islet cells as the db+STZpio mice had blood sugars reduced almost to normal. We designed a small pilot study to see if starting with older mice and delaying the pioglitazone treatment for several weeks after STZ injections would allow the mice to live longer.

We started with 6 db+ males at 8 wks age who had been fed standard LabDiet 5053 chow. They received injections of 150 mg/kg STZ, at 8 wks age, then we waited either 2 or 3 weeks to start pio chow treatment. All the mice had high fasting glucoses (average 556 mg/dL) within 1 week of STZ injections. Weights and fasting glucoses were measured weekly. Fasting glucoses remained high throughout the study. All mice died within 2 weeks of starting pio chow treatment, and those mice that began pio chow treatment later (at 3 wks post-STZ) all died within 1 week of switching to pio chow. At this point, we are unsure why this group of mice responded so poorly to pio chow treatment, but we suspect that the pio chow was not palatable to these older diabetic mice, perhaps due to its harder consistency. We plan to repeat a similar small pilot study where we start the mice early on the control base chow (AIN76A) at 5 wks age to acclimate them to the consistency of the base chow, give STZ injections at 5 or 8 wks age, start pio chow treatment (AIN76 + pioglitazone) at 10 or 11 wks age. We also plan on putting moist chow on the floor of the cage daily.

<u>Neuropathy in a Genetic Mouse Model of Dyslipidemia</u>

Introduction

As discussed above, our ongoing hypothesis is that plasma lipids contribute a key role in the development of DPN. In order to assess the role of dyslipidemia distinct from hyperglycemia in the development of neuropathy, we have characterized two different models of dyslipidemic triple knockout (3KO) mice; $ApoE^{-/-}$/$ApoB^{100only}$/ob/ob (ApoE 3KO) and $LDLR^{-/-}$/$ApoB^{100only}$/ob/ob (LDLR 3KO). We have completed preliminary phenotyping of both mice at 24 wk of age.

ApoE 3KO Mice: These mice are obese and develop diabetes and diabetic neuropathy (Fig. 18). However, we identified a number of weaknesses in this mouse model for the purposes of this study. Their hyperglycemia began to decrease after 16 wk of age and became more variable. The lipid profiles indicate that there is only a modest, 2-fold, increase in plasma cholesterol and no increase in plasma triglycerides at 24 wk of age. Because these mice neither develop hyperlipidemia nor maintain hyperglycemia in a manner that we can readily regulate, we are focusing on the LDLR 3KO mice for mechanistic studies.

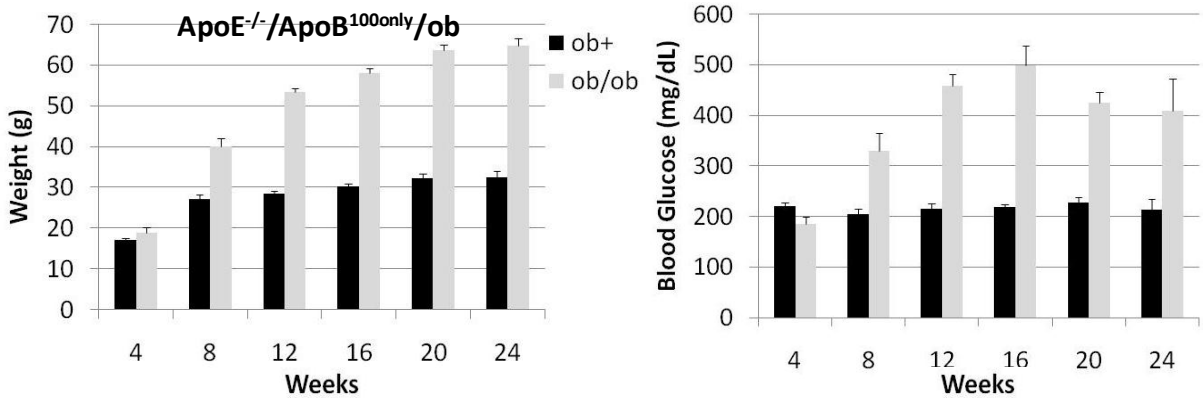

	Insulin (ng/ml)	GHb (%)	Chol. (mg/dl)	Trig (mg/dl)	Von Frey (g)	Hind Paw (s)	Tail Flick (s)	Sural (m/s)	Sciatic (m/s)
ob+	0.91±0.16	8.25±0.4	237.8±15.7	114.3±17.4	2.5±0.3	3.7±0.3	3.9±0.3	23.27±0.75	57.27±1.45
ob/ob	10.94±3.06	13.09±0.9	500.2±42.1	122.4±22.2	6.7±0.9	5.1±0.5	5.3±0.3	19.3±1.02	41.80±1.74

Fig. 18. ApoE 3KO Mouse Phenotype. Body weight (left panel) and fasting glucose (right panel) were measured every 4 wk up to 24 wk. Plasma insulin, glycated hemoglobin (GHb), total cholesterol and triglycerides were measured at 24 wk, as were mechanical and thermal sensitivity and NCV.

LDLR 3KO Mice: In contrast to ApoE 3KO mice, the LDLR 3KO mice demonstrate the metabolic parameters that permit testing our main hypothesis that dyslipidemia contributes to neuropathy. The metabolic profiles of the LDLR/ApoB^{100only}/ob/+ and LDLR/ApoB^{100only}/ob/ob mice are shown in Fig. 19. Although the LDLR 3KO mice are as obese as the ApoE 3KO mice, they do not display hyperglycemia (Fig. 19A). We also took random blood glucose measures at 20-24 wk and these were 169±8 mg/dl in LDLR/ApoB^{100only}/ob/+ and 174±10 mg/dl in LDLR/ApoB^{100only}/ob/ob mice. The LDLR 3KO mice were hyperinsulinemic and their glycated hemoglobin (GHb) was not significantly elevated. Most notably, the LDLR 3KO mice were hyperlipidemic. Total plasma cholesterol (Chol) and triglycerides (Trig) were increased approximately 4-fold in 3KO compared with LDLR/ApoB^{100only}/ob/+ mice (Fig. 19B). FPLC fractionation of the plasma revealed that these lipids were mostly partitioned in the VLDL and LDL, with a 2-fold increase in HDL cholesterol.

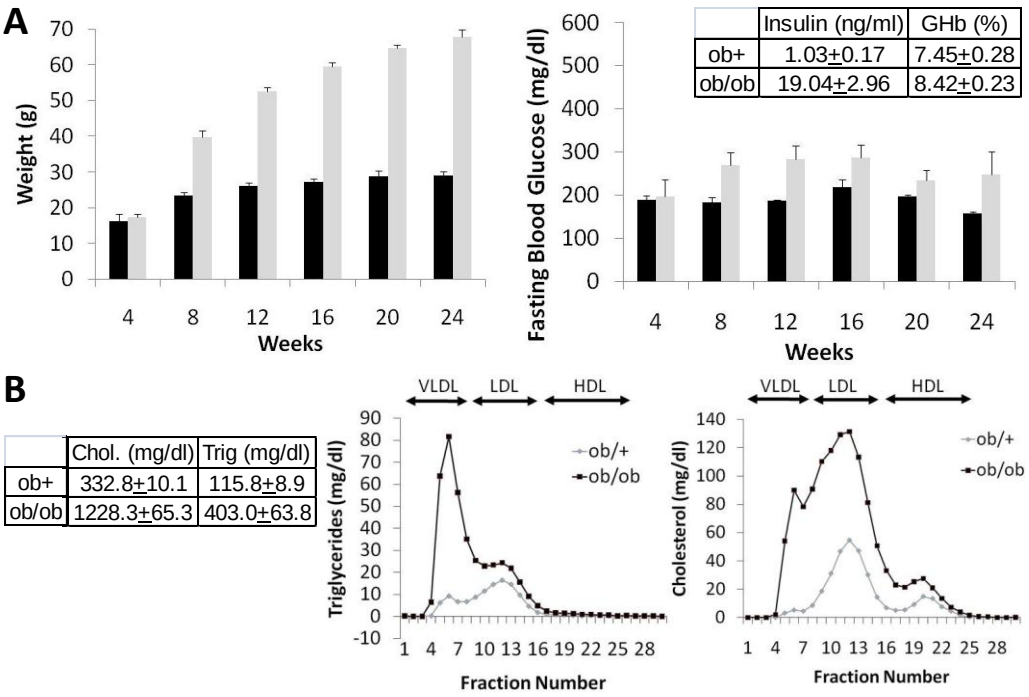

Fig. 19. Blood Glucose & Lipids in LDLR 3KO Mice. (A) Glycemia control. Body weight and fasting glucose were measured every 4 wk up to 24 wk when plasma insulin and glycated hemoglobin (GHb) were measured. The bar graph indicates that LDLR 3KO mice are obese compared to ob/+ littermates but they are not diabetic (fasting blood glucose is not > 300 mg/dL). The mice exhibit hyperinsulinemia but GHb is not significantly elevated. (B) Plasma lipids, total triglycerides and cholesterol were measured in whole plasma and in plasma fractionated by FPLC (performed at University of Washington Mouse Metabolomic Phenotyping Core).

We assessed behavioral evidence of neuropathy in the LDLR 3KO mice and their ob/+ littermates at 16 and 24 wk of age and NCV and sural nerve fiber loss at 24 wk of age (Fig. 20). At 16 wk, LDLR 3KO mice demonstrate a modest increase in hind paw latency, but no significant difference in response to Von Frey fibers or tail flick when compared with ob/+ littermates. At 24 wk, neuropathy is evident via all three parameters (Fig. 20). This suggests that there is a slower onset of neuropathy in dyslipidemia alone than that seen in the presence of diabetes (compare with db/db mice (Sullivan et al. 2007)). The sciatic and sural NCV were significantly decreased at 24 wk. Finally, we demonstrate a loss of sural nerve fibers in the LDLR 3KO mice compared with ob/+ littermates. These data provide strong evidence that dyslipidemia alone causes neuropathy in mice and demonstrate our progress in establishing this model for mechanistic investigations. In addition to counting the total number of nerve fibers, we measure fiber diameter and myelin thickness and integrity using MetaMorph software. In these single representative LDLR 3KO and ob/+ littermate images, we observe a decrease in the largest fibers.

Summary

These data demonstrate that we can explore the mechanisms of dyslipidemia-induced neuropathy in the LDLR 3KO mice. We are currently examining the oxLDL-LOX-1 axis in these mice at 16 and 24 wk of age as well as the therapeutic potential of fenofibrate (activation of PPARα) to prevent neuropathy.

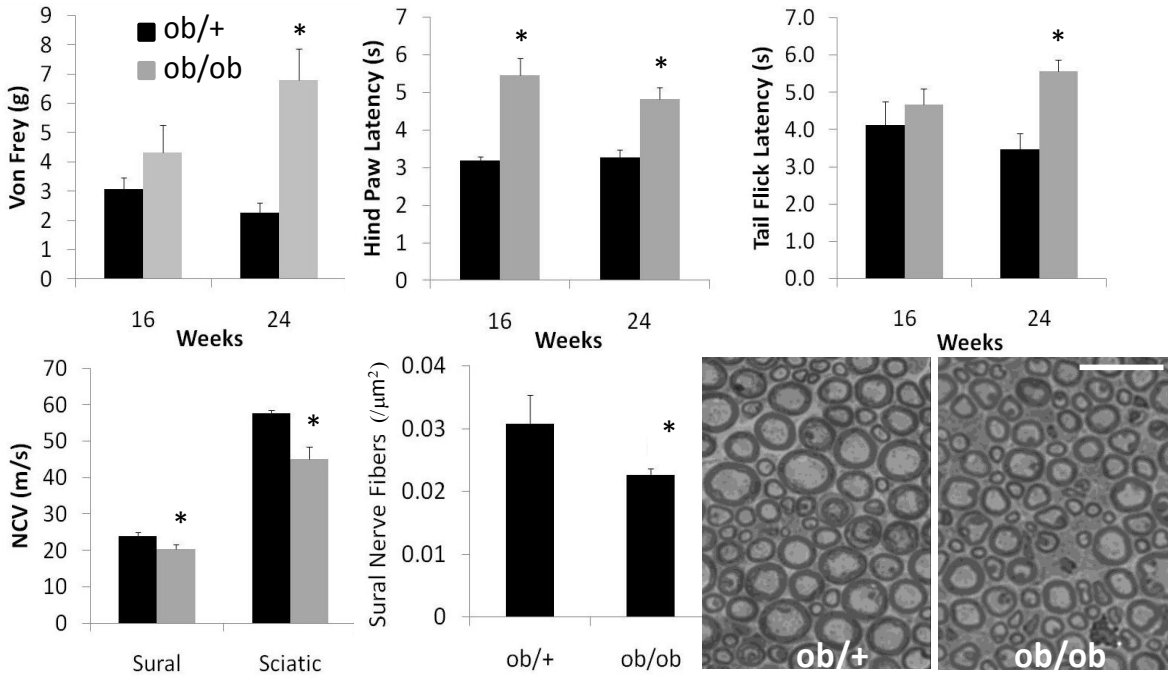

Fig. 20. Neuropathy phenotyping in LDLR 3KO mice. Mechanical and thermal sensitivity testing were performed at 12 and 24 wk of age, while NCV and sural nerve fiber density were measured at 24 wk only. $p<0.05$ when comparing ob/+ and ob/ob littermates. For sural nerve analyses, the total number of fibers across an entire cross-section of the nerve were counted and normalized per cross-section area. The images are representative samples from the middle of the nerve. Bar = 50 μm.

Evidence for the Role of LOX-1 in Dyslipidemia-Induced Neuropathy *in Vivo*

Introduction

Our preliminary hypothesis regarding dyslipidemia and neuropathy was that DRG neurons interact with lipids. Since diabetes is associated with increased oxidative stress, we focused on oxidized lipoproteins, specifically oxidized low density lipoproteins (oxLDL). We examined the role of a known vascular oxLDL receptor known as LOX-1. We demonstrated *in vitro* that DRG neurons express LOX-1 and that interaction with oxLDL produced both cellular redox signaling and oxLDL uptake that injures the neurons (Vincent et al, Diabetes 58:2376-2685, 2009). Next, we wanted to demonstrate this mechanism *in vivo*.

Methods and Results

First, we examined the expression of LOX-1 in DRG of LDLR 3KO mice and their $LDLR^{-/-}$/$ApoB^{100only}$/ob+ littermates (Fig 21). LOX-1 was present on the DRG of non-dyslipidemic $LDLR^{-/-}$/$ApoB^{100only}$/ob+ mice but was markedly increased in the LDLR 3KO (ob/ob) mice at 24 wk of age. In a new pilot study, we sought direct evidence that LOX-1 is involved in the development of neuropathy. We neutralized LOX-1 activity *in vivo* using a specific antibody. We injected I.P. with 100 μL of 1.6 μg/mL protein in saline of either goat anti-mouse LOX-1 (R&D Systems) or control nonimmune goat IgG. Injections were every other day from 6 to 12 wk of age and

terminal phenotyping was performed at 12 wk of age. Because we are still breeding 3KO mice for metabolic phenotyping at 16 wk and for the fenofibrate study, we turned to db/db mice that are more readily available and are well-characterized in our laboratory. We find that neutralization of LOX-1 produces a modest decrease in blood glucose without altering weight gain (Fig. 22) and no change in total plasma triglycerides or cholesterol (not shown), but these mice remain diabetic (fasting glucose around 400 mg/dL). Treatment of db/db mice with anti-LOX-1 preserved the sural NCV when compared with treatment with non-immune IgG (Fig. 22). The diabetes-induced defect in sciatic motor NCV (SMNCV) was not different between IgG or anti-LOX-1 treatments.

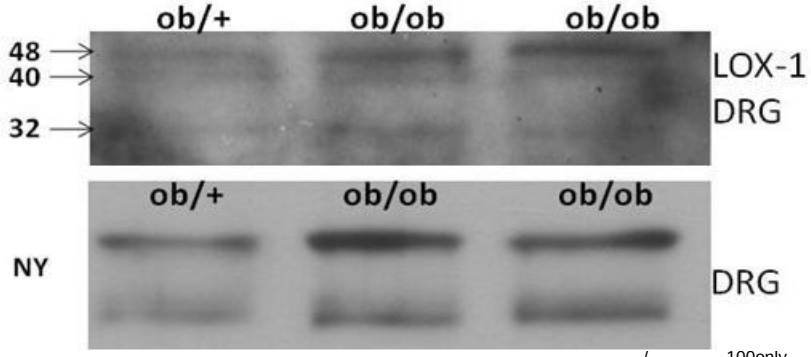

Fig. 21. Expression of LOX-1 and related proteins in mice. LDLR$^{-/-}$/ApoB^{100only}/ob/+ or LDLR$^{-/-}$/ApoB^{100only}/ob/ob mice were euthanized and tissues harvested at 24 wk of age and 15 μg DRG was subjected to Western blotting HC. We blotted for LOX-1 or nitrotyrosine (NY). The cell surface (48 kDa) isoform of LOX-1 was increased in dyslipidemic LDLR$^{-/-}$/ApoB^{100only}/ob/ob mice compared to non-dyslipidemic LDLR$^{-/-}$/ApoB^{100only}/ob/+ littermates.

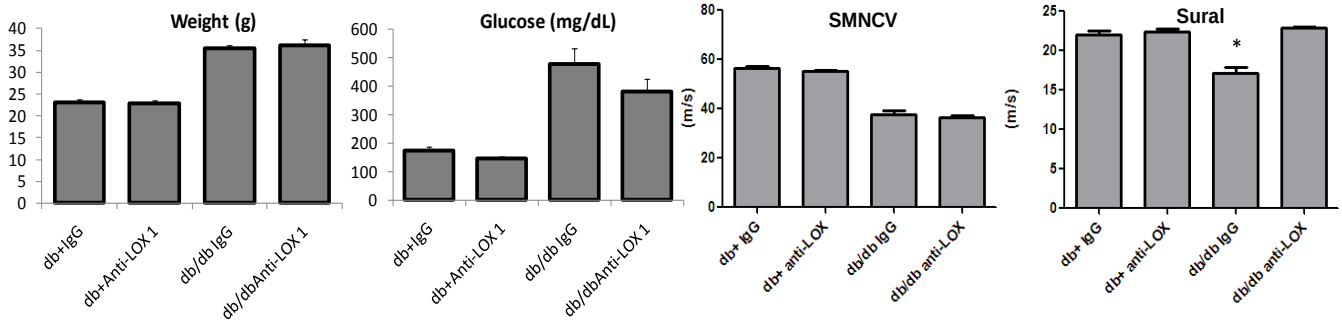

Fig. 22. Blocking LOX-1 decreases sural NCV defects in db/db mice. db/+ and db/db mice (n=6 per group) were *Sural NCV was significantly decreased in db/db mice treated with IgG ($p<0.05$) but preserved with anti-LOX-1 treatment. Mice were euthanized and plasma, whole blood, DRG, sciatic nerves, and hind footpads were harvested for morphological phenotyping. These tissues are being processed at the time of submission.

Summary

This data demonstrate a specific role for DRG (and potentially microvascular) LOX-1 in the development of neuropathy *in vivo* and we will continue to analyze these mice. Since the sciatic NCV deficit was not prevented by LOX-1 inhibition, we underscore the complex interplay of metabolic imbalances that contribute to diabetic neuropathy. We anticipate that we will find more complete protection by LOX-1 inhibition in the LDLR 3KO mice.

Collaborations

AMDCC collaborations:

In the past year we collaborated with 5 different AMDCC investigators.

Drs. Brosius/Kretzler (University of Michigan)

Our primary collaboration is with Drs. Frank Brosius and Matthias Kretzler, as we continue to phenotype all diabetic nephropathy mouse models for DPN. This productive collaboration has lead to not only a series of publications but also a recently funded R24 application where we will use a systems biology approach to identify potential therapeutic targets in common between the two complications (NIH 1 R24 DK082841-01 09/01/09 - 09/29/14 Integrated Systems Biology Approach to Diabetic Microvascular Complications). We are currently collaborating on 2 models: Akita mice in a PodoCreJak-2 study on 129 s6Tac mice and eNOS KO BKSdbdb/db+ mice.

Dr. Smithies (University of NC)

We continue to collaborate with and phenotype mice for the Smithies group. Our data were published last year and we will continue this productive collaboration as appropriate models are generated.

Dr. Elizabeth Leibold (University of Utah)

We completed complete neuropathy phenotyping on IRP2 KO mice (n=16) received from Dr. Leibold at the University of Utah. Her group is interested in mechanisms regulating mammalian iron homeostasis by the iron regulatory protein 2 (IRP2). IRP2 is a RNA-binding protein that posttranscriptionally regulates the translation or stability of mRNAs encoding iron homeostasis proteins, such as ferritin, transferrin receptor, HIF-2alpha and several other proteins. IRPKO mice develop mild neurodegenerative disease (locomotor and balance problems) and is associated with altered brain iron. She recently found that these mice develop diabetes by 2 months of age, which is due to reduced beta cell function and mass, leading to reduced insulin content. Nociception tests (hot plate) revealed that IRP2KO mice (males and females, 5-month and 12-month old mice) showed significant longer hind paw licking , but no difference in hind paw shaking. These data suggested the possibility that hypolagesia in IRP2KO mice might be due impaired glucose tolerance. At her request, we performed impaired glucose tolerance testing, assayed Von Frey fiber, tail flick, hind paw withdrawal, nerve conduction velocity testing and IENF density. We harvested DRG, sciatic nerve, sural nerve, spinal cord, and footpad to further examine any biochemical alterations. We also harvested pancreas at Dr. Leibold's request and returned the tissue to her lab. We remain blinded as to the genotypes of her mice.

Dr. Richard Davis (UCLA)

We received footpads from several of Dr. Davis' models and have completed IENF counts. Unfortunately, we did not detect any statistical differences, suggesting there is not a significant DPN in these murine models.

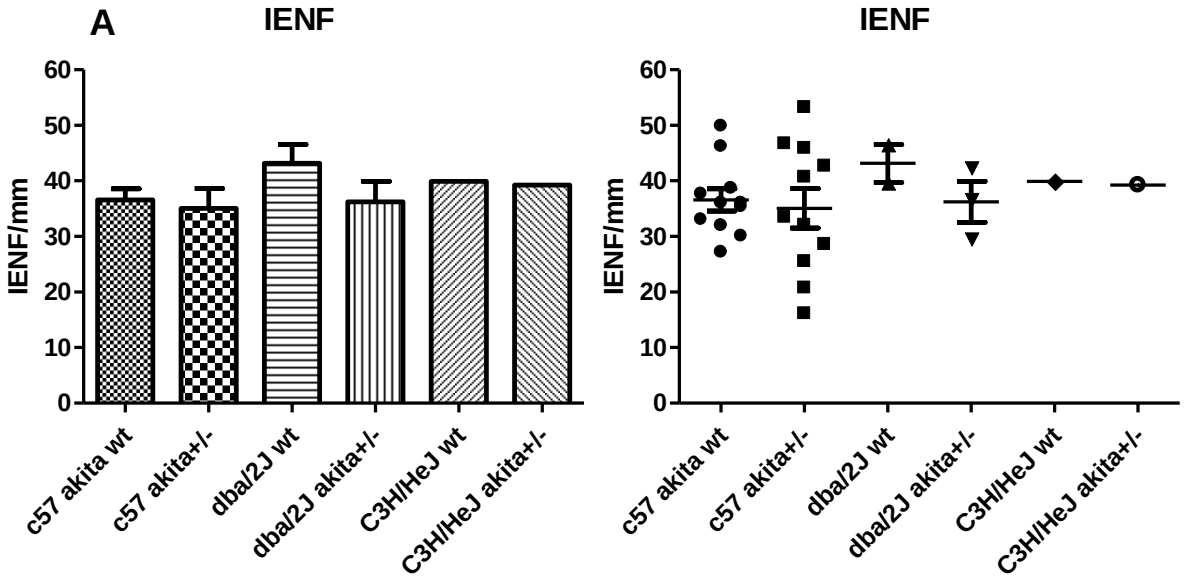

Figure 18. IENF counts in mouse models from Richard Davis. We did not see any difference between the C57BL/6J Akita wild type and the C57BL/6J Akita het. The number of samples is too low with the other genotypes to make a determination. The genotype is either +- (Heterozygous for the Akita Mutation: Diabetic) or wt (Wild type). Most of the animals in the study are F1 hybrids between B6 and the indicated strain (in this case, A/J, C3H and DBA). The C57BL/6 animals are pure B6.

Jackson Lab Collaboration:

We received BTBR KO-obob and BTBR KO-ob+ female mice at age 26 wks from Jackson lab (in collaboration with Dr. Charles Alpers) and performed terminal neuropathy phenotyping, including TF, HP, Sural NCV and SMNCV, and collected tissue for exploration of biochemical alterations in DRG, sciatic nerve, sural nerve, spinal cord, footpad and brain.

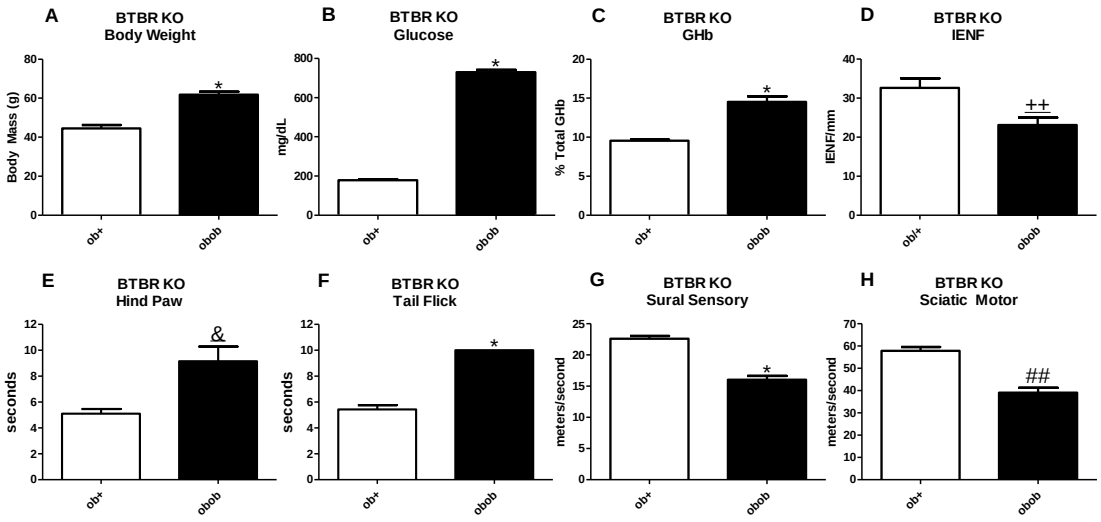

Figure 19. Data represent 26 week old BTBR KO-obob and BTBR KO-ob+ mice.
(A) Body weight, (B) fasting glucose, (C) GHb (glycosylated hemoglobin), and (D) intraepidermal nerve fibers were all significantly altered in 26 week old BTBR KO-obob mice compared to BTBR KO-ob+ mice. *P<.0001, $^{++}$P=.0163. There was a significant increase in latency in the HP (E) as well as the TF (F) in BTBR KO- obob mice. *P<.0001, $^{\&}$P=.0069. Additionally, there was a pronounced reduction in Sural NCV (G) and SMNCV (H) at 26 weeks of age in BTBR KO- obob mice. *P<.0001, $^{\#\#}$P=.0002. N=5/group and two tail t-test with a 95% confidence interval. Data are expressed as means $\pm$ SEM.

MMPC collaboration:
University of Washington MMPC core:
We sent 204 plasma samples in 2010 for FPLC, total cholesterol, total triglycerides and insulin measurements.

Non-AMDCC collaborations:

Dr. Ahmet Hoke (Johns Hopkins University)

We continued exploring the role of mitochondrial (Mt) biology in animal models of type 2 diabetes with our ongoing collaboration with Dr. Hoke.
BKS-dbdb and db+ mice (BKS.Cg-m +/+ Leprdb/J, JAX Mice stock # 000642) were purchased from Jackson Laboratory (Bar Harbor, ME) and used as a model of type 2 diabetes. Mice were aged to 24 wks, tissue harvested and sent to Dr. Hoke to examine mtDNA mutations in DRG, sciatic nerve and sural nerve.

His lab performed a mtDNA deletion assay using nested PCR. Since the short DNA can be amplified much more effectively under the designed amplification conditions, the fluorescence reading represents mostly the amplification of mitochondrial DNA with large deletion(s). Ratio of this amplified PCR product fluorescence reading to internal control PCR product fluorescence reading was used to compare the quantity of the original mitochondrial

genomic DNA templates with deletions. All primers were designed according to the published mouse mitochondrial genome (Bibb et al: Sequence and gene organization of mouse mitochondrial DNA. Cell 26:167-180, 1981)

There is a significant difference in the mtDNA mutations between control and DPN groups only in the sural nerves. The sciatic nerve did not give a difference as there was a bigger variability among the samples. This is something Dr. Hoke has seen with monkey nerves as well, perhaps due to fact that sciatic has motor nerves as well.

As part of this collaboration focusing on the sural nerve, we counted the total number of axons in the sural nerves of 24 wk BKSdbdb and db+ mice.

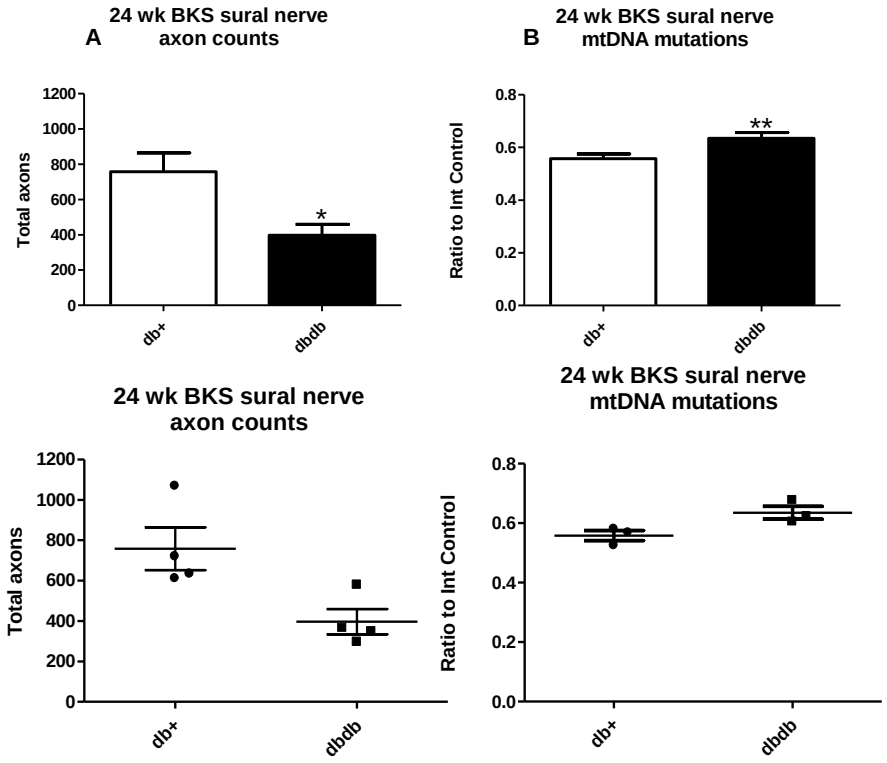

Figure 20. Sural nerve analysis from 24 wk old mice. (A) Total number of axons were significantly reduced in the distal segment of sural nerve in dbdb mice compared to db+ mice , *p value = .0490. (B) The ratio of mitochondrial DNA mutations significantly increased in dbdb sural nerve when compared to db+ sural nerve, ** p value = .0262. A two tailed t-test was used with a 95% confidence level. Data are expressed as means ± SEM

Dr. Dan Michele (University of Michigan)

We completed tail flick assays and nerve conduction velocity testing on a mouse model of congenital muscular dystrophy for Dr. Michele. His mouse model of congenital muscular dystrophy has specifically rescued the gene defect in skeletal muscle, and his lab is trying to understand the contribution of peripheral neuropathy to the muscle dysfunction in this disease.

The mice eventually get a hind limb paralysis after about 6-8 months of age which is believed to be due to a peripheral neuropathy but is not definitively proven.

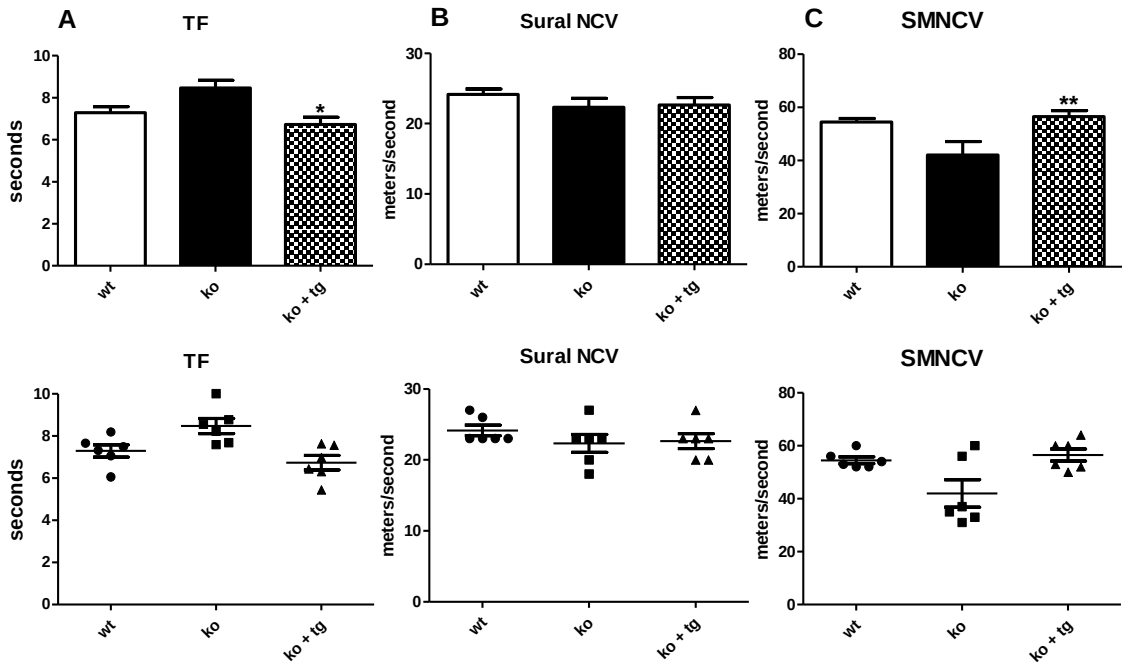

Figure 21. Neuropathy phenotyping . Comparing mice with the myd mutation (ko) to mice with myd mutation with a rescue transgene (ko+tg), the TF (A) and the SMNCV (C) were restored to normal values with the rescue transgene. The transgene had no effect on the other measurements. *P=.05, **P=.01. A one way ANOVA and a Tukey post-hoc test with a 95% confidence level was used for analysis. N=6/group. . Data are expressed as means± SEM.

Dr. Antonetti, Dr. Gardner, Dr. Abcouwer (University of Michigan Kellogg Eye Center)

We began to collaborate with our colleagues at the University of Michigan Kellogg Eye Center to further explore retinopathy in our mouse models of type 2 diabetes. We provided eyes from the mice in our pioglitazone study and several BKS-dbdb/db+ studies (16 wk age, 24 wk age) to them for analysis of retinopathy and will continue to provide eyes from future models of interest.

1. **Address previous EAC comments:**

Please address each comment

- The annual report reviewed work on mitochondrial responses to hyperglycemia *in vivo* and *in vitro*, visualization of mitochondrial biogenesis, effects of anesthesia on nerve conduction velocity, mechanical allodynia and p38, and insulin resistance in cortical neurons. All of the work appeared interesting, important and well along. The major issue that could be raised is how well the current directions fit the overall theme of AMDCC. While of valuable scientific interest, it is not clear the work in general emphasizes model development.

The investigation of mechanical allodynia and p38 is part of our ongoing development of mouse models of neuropathic pain. This particular area of DPN is under studied, especially in type 2 animal models.

Dr. Bhumsoo Kim has an ongoing interest in models of Alzheimer's disease. We provided Dr. Kim with brains from BKS db/db mice harvested as part of our examinations of DPN. No extra costs were incurred and his work is expanding our knowledge of the effects of hyperglycemia, dyslipidemia and pathology of the central nervous system.

- It was unclear whether all of this work was specific AMDCC work, evaluating new models of diabetic neuropathy, particularly as they relate to mitochondrial function, or reflected general work in the laboratory of the investigator. This is particularly the case with the *in vitro* work, which is a step away from evaluating specific models.

All animal work on DPN performed within the laboratory is funded by the AMDCC. We have reported changes in mitochondrial morphology and biogenesis in both *in vivo* and *in vitro* models. We include data derived from our *in vitro* analyses as a guide for our *in vivo* studies and use these experiments to confirm and extend questions regarding the mechanisms underlying DPN.

- Mitochondrial biogenesis: It would be helpful to define the functional significance, axon subtype specificity, axon vs. DRG involvement. What AMDCC models will this be relevant to?

Mitochondrial fission, fusion and biogenesis are mechanisms by which energy load is distributed and new mitochondria replace the old. We believe that mitochondrial disruption is an inherent mechanism driving the death of sensory neurons and the dying back of peripheral neurites. Therefore, we feel that mitochondrial deficits contribute to both type 1 and 2 models of DPN. We are currently examining potential differences in mitochondrial morphology in DRG neurons and sural nerves.

- What is your hypothesis with regard to the effect of anesthesia on nerve conduction? Why investigate surface temperatures when maintenance of core temperature is essential to properly control nerve conduction results? Probably best to internally choose an anesthetic and stick with it in experimental mice and controls. Novelty of this section not high.

Our goal in performing this study was to discover which anesthesia had the least impact on measures of nerve conduction and the most consistent dosing and recovery. We realize that this work is not exciting but without documentation of our findings, it would be difficult to convince other groups to use isoflurane rather than pentobarbital or ketamine. It was also important for us to examine multiple sessions of anesthesia as repeated NCV measures are difficult in diabetic mice, mainly due to anesthetic overdose.

- No information is submitted on the progress of SOD mice.

This information is included in the current report.

- How does the work on insulin resistance tie into AMDCC goals and relevance? P38 work is well done and interesting. Why is the focus on TrkA cells only? What about thermal hyperalgesia?

The work on insulin resistance in cortical neurons was performed by Dr. Bhumsoo Kim, an Assistant Research Professor in Dr. Feldman's laboratory. These experiments were performed in parallel with our DPN studies and while not directly related to DPN, are related to the complications of diabetes. The risk of developing Alzheimer's disease increases significantly in type 2 diabetic patients. In addition, insulin is a known growth factor for peripheral as well as central neurons. It is not yet clear whether insulin resistance contributes to the development of DPN but this presents an intriguing possibility.

As mentioned above, p38 and TrkA neurons are implicated in the development of neuropathic pain associated with the early phase of DPN. We have reported changes in thermal sensitivity, the BKSdbdb mouse exhibits thermal allodynia at approximately 8 weeks of age (4 weeks of diabetes).

- Minor question: Is sural nerve conduction in mice the proper terminology?

Yes

- Drs. Smithies and Feldman should be commended for their efforts to cross phenotype models.

Thank you.

- Dr. Feldman's group continues to be highly productive and generates new and important data. Dr. Feldman is also very responsive in addressing suggestions.

Thank you.

- It is great to see these mechanistic studies coming out of the initial model development.

We agree and are excited about pursuing these studies.

- Since glitazones are widely used to treat T2D, the planned study to look at their effect on neuropathy should yield important data.

Yes, and a preliminary study is presented above. As mentioned, the early application of pioglitazone may have partially restored islet cell function. Another study is currently underway to better examine the effects of a TZD on DPN in both type 1 and 2 models.

- Dr. Maeda's models should be tested for neuropathy if it isn't being done already.

This work is underway.

- The website is set-up to display microarray data. Has all of the data from your P&F award (with Dr. Kretzler) been uploaded to the site?

Yes.

- The overall goal of this project is to understand the role of oxidative stress and mitochondrial dysfunction on diabetic neuropathy. The progress for the current year is outstanding, and the PI has been highly productive. The PI has addressed all of the concerns of the panel from last year regarding collaborations with new AMDCC investigators. The PI continues to expand the scope of the project and shows an impressive amount of data and progress. The project remains highly innovative, and the productivity is impressive.

Thank you, being part of the AMDCC has given my laboratory the opportunity to perfect and refine our methods and examine new animal models. We all look forward to future collaborations with the group.

Publications citing current NIH grant (names in bold are AMDCC members):

Sims-Robinson C, Kim B, Rosko A, **Feldman EL**. How does diabetes accelerate Alzheimer disease pathology? *Nat Rev Neurol.* 2010 Oct. 6(10):551-9. PMID: 20842183

Hur J, Sullivan KA, Schuyler AD, Hong Y, Pande M, States DJ, Jagadish HV, **Feldman EL.** Literature-based discovery of diabetes- and ROS-related targets. *BMC Med Genomics*. 2010 Oct 27: 3:49. PMID: 20979611

Oh SS, Hayes JM, Sims-Robinson C, Sullivan KA, **Feldman EL.** The effects of anesthesia on measures of nerve conduction velocity in male C57Bl6/J mice. *Neurosci Lett*. 2010 Oct 11;483(2):127-31. PMID: 20691755

Kakoki M, Sullivan KA, Backus C, Hayes JM, Oh SS, Hua K, Gasim AM, Tomita H, Grant R, Nossov SB, Kim HS, Jennette JC, **Feldman EL**, **Smithies O**. Lack of both bradykinin B1 and B2 receptors enhances nephropathy, neuropathy, and bone mineral loss in Akita diabetic mice. *Proc Natl Acad Sci U S A*. 2010 Jun 1;107(22):10190-5. PMID: 20479236

Vincent AM, Edwards JL, McLean LL, Hong Y, Cerri F, Lopez I, Quattrini A, **Feldman EL**. *Mitochondrial biogenesis and fission in axons in cell culture and animal models of diabetic neuropathy. Acta Neuropathol.* 2010 Oct;120(4):477-89. PMID: 20473509

Pop-Busui R, Roberts L, Pennathur S, **Kretzler M**, **Brosius FC, Feldman EL**. The management of diabetic neuropathy in CKD. *Am J Kidney Dis*. 2010 Feb;55(2):365-85. PMID: 20042258

Vincent AM, Hinder LM, Pop-Busui R, **Feldman EL**. Hyperlipidemia: a new therapeutic target for diabetic neuropathy. J *Peripher Nerv Syst.* 2009 Dec;14(4):257-67. PMID: 20021567

Below is a list of your AMDCC publications from the website. Should any publications be added or subtracted? Has all of the relevant data from these publications been uploaded to the website? Please work with Dr. Rick McIndoe to ensure that the website and database are up-to-date and complete.

1. The management of diabetic neuropathy in CKD.
   Pop-Busui R, Roberts L, Pennathur S, Kretzler M, Brosius FC, Feldman EL
   American journal of kidney diseases : the official journal of the National Kidney Foundation, 2010 (55(2)), 365 - 385
2. Hyperlipidemia: a new therapeutic target for diabetic neuropathy.
   Vincent AM, Hinder LM, Pop-Busui R, Feldman EL
   Journal of the peripheral nervous system : JPNS, 2009 (14(4)), 257 - 267
3. Increased tau phosphorylation and cleavage in mouse models of type 1 and type 2 diabetes.
   Kim B, Backus C, Oh S, Hayes JM, Feldman EL
   Endocrinology, 2009 (150(12)), 5294 - 5301
4. Nerve Growth Factor Mediates Mechanical Allodynia in a Mouse Model of Type 2 Diabetes
   Hsinlin T Cheng, John M Hayes, Yu Hong and Eva L Feldman
   Journal of neuropathology and experimental neurology, 2009
5. SUMOylation of the mitochondrial fission protein Drp1 occurs at multiple nonconsensus sites within the B domain and is linked to its activity cycle.
   Figueroa-Romero C, Iñiguez-Lluhí JA, Stadler J, Chang CR, Arnoult D, Keller PJ, Hong Y, Blackstone C, Feldman EL

The FASEB journal : official publication of the Federation of American Societies for Experimental Biology, 2009 (23(11)), 3917 - 3927
6. Dyslipidemia-Induced Neuropathy in Mice: the Role of oxLDL/LOX-1
   Andrea M. Vincent, John M. Hayes, Lisa L. McLean, Anuradha Vivekanandan-Giri, Subramaniam Pennathur, and Eva L. Feldman
   Diabetes, 2009 (58(10)), 2376 - 2385
7. Computational methods for predicting sites of functionally important dynamics.
   Schuyler AD, Carlson HA, Feldman EL
   The journal of physical chemistry. B, 2009 (113(19)), 6613 - 6622
8. Hydrogen peroxide-induced Akt phosphorylation regulates Bax activation.
   Sadidi M, Lentz SI, Feldman EL
   Biochimie, 2009 (91(5)), 577 - 585
9. Loss of myotubularin function results in T-tubule disorganization in zebrafish and human myotubular myopathy.
   Dowling JJ, Vreede AP, Low SE, Gibbs EM, Kuwada JY, Bonnemann CG, Feldman EL
   PLoS genetics, 2009 (5(2)), e1000372
10. Insulin-like growth factors in the peripheral nervous system.
    Sullivan KA, Kim B, Feldman EL
    Endocrinology, 2008 (149(12)), 5963 - 5971
11. Mechanisms of disease: the oxidative stress theory of diabetic neuropathy.
    Figueroa-Romero C, Sadidi M, Feldman EL
    Reviews in endocrine & metabolic disorders, 2008 (9(4)), 301 - 314
12. Rosiglitazone reduces renal and plasma markers of oxidative injury and reverses urinary metabolite abnormalities in the amelioration of diabetic nephropathy
    Hongyu Zhang, Jharna Saha, MaryLee Schin, Jaeman Byun, Matthias Kretzler, Eva L. Feldman, David A. Weild, Subramaniam Pennathur, Frank C. Brosius III
    American journal of physiology. Renal physiology, 2008 (295(4)), F1071 - F1081
13. Kindlin-2 is required for myocyte elongation and is essential for myogenesis.
    Dowling JJ, Vreede AP, Kim S, Golden J, Feldman EL
    BMC cell biology, 2008 (9), 36
14. Rosiglitazone Treatment Reduces Diabetic Neuropathy in STZ treated DBA/2J mice
    Timothy D Wiggin, Matthias Kretzler, Subramaniam Pennathur, Kelli A. Sullivan, Frank C Brosius, Eva L Feldman
    Endocrinology, 2008 (149(10)), 4928 - 4937
15. From fibrosis to sclerosis: mechanisms of glomerulosclerosis in diabetic nephropathy.
    Qian Y, Feldman E, Pennathur S, Kretzler M, Brosius FC
    Diabetes, 2008 (57(6)), 1439 - 1445
16. National Institute of Diabetes and Digestive and Kidney Diseases (NIDDK) meeting summary Advances toward measuring diabetic retinopathy and neuropathy: from the bench to the clinic and back again (April 4-5, 2007, Baltimore, Maryland).
    Kern TS, Berkowitz BA, Feldman EL
    Journal of diabetes and its complications, 2008 ([Epub ahea)
17. Membrane traffic and muscle: lessons from human disease.
    Dowling JJ, Gibbs EM, Feldman EL
    Traffic (Copenhagen, Denmark), 2008 (9(7)), 1035 - 1043
18. Criteria for creating and assessing mouse models of diabetic neuropathy.
    Sullivan KA, Lentz SI, Roberts JL, Feldman EL
    Current drug targets, 2008 (9(1)), 3
19. SOD2 Protects Neurons from Injury in Cell Culture and Animal Models of Diabetic Neuropathy
    Andrea M. Vincent, James W. Russell, Kelli A. Sullivan, Carey Backus, John M. Hayes,

Lisa L. McLean and Eva L. Feldman
Experimental neurology, 2007 (208), 216 - 227

20. Mouse models of diabetic neuropathy.
Sullivan KA, Hayes JM, Wiggin TD, Backus C, Su Oh S, Lentz SI, Brosius F, Feldman EL
Neurobiology of disease, 2007 (28(3)), 276 – 285